SOIL CONSTITUENT PATTERNS AND PREDICTIONS USING VNIR CALIBRATIONS AND ANALYSES OF SOIL MAP UNITS ACROSS SLOPE STEEPNESS UNDER LONGLEAF PINE ECOSYSTEMS

by

JENNA CHRISTINE STOCKTON

(Under the Direction of Daniel Markewitz)

ABSTRACT

Visible/near-infrared scans on a range of soil series under longleaf pine (*Pinus palustris*) were calibrated with soil total carbon using different methods to assess measurement accuracy. Soil data for 900 samples were provided by the Natural Resources Conservation Service. Spectra were preprocessed using three methods; Savitzky-Golay (SG), continuum removal, and wavelets. Two multivariate algorithms, the partial least square regression and support vector machine (SVM), were used to determine the best calibration model based on the coefficient of determination (R^2). The SVM algorithm combined with the SG transformation provided the best calibration and validation prediction at a $R^2 = 0.70$ for mineral soils. Adjoining soil map units that vary in slope steepness were also analyzed for that vary in slope steepness with soil property patterns at four different sites in GA. Few significant differences were observed with slope steepness at any depth (0-200 cm) for the measured variables (percent clay, C, pH).

VNIR calibrations for percent clay demonstrated potential predictive value (i.e., $R^2 \geq 0.9$) while those for C and pH_{cacl2}, although not as strong (i.e., $R^2 \geq 0.67$ and $R^2 \geq 0.54$, respectively), indicated some utility for field classification or monitoring of dynamic soil properties under longleaf pine ecosystems.

INDEX WORDS: Visible/Near-Infrared Spectroscopy, Multivariate Calibrations, Pre-processing Transformations, Soil Total C, Soil Map Units, Slope, Longleaf Pine

SOIL CONSTITUENT PATTERNS AND PREDICTIONS USING VNIR CALIBRATIONS AND ANALYSES OF SOIL MAP UNITS ACROSS SLOPE STEEPNESS UNDER LONGLEAF PINE ECOSYSTEMS

by

JENNA CHRISTINE STOCKTON

B.S., University of Mary Washington, 2014

A Thesis Submitted to the Graduate Faculty of The University of Georgia in Partial Fulfillment of the Requirements for the Degree

MASTER OF SCIENCE

ATHENS, GEORGIA

2016

SOIL CONSTITUENT PATTERNS AND PREDICTIONS USING VNIR CALIBRATIONS AND ANALYSES OF SOIL MAP UNITS ACROSS SLOPE STEEPNESS UNDER LONGLEAF PINE ECOSYSTEMS

by

JENNA CHRISTINE STOCKTON

Major Professor:	Daniel Markewitz
Committee:	JP Schmidt
	Lawrence Morris
	William Miller

Electronic Version Approved:

Suzanne Barbour
Dean of the Graduate School
The University of Georgia
December 2016

ACKNOWLEDGEMENTS

I would like to extend many thanks to my major advisors, Daniel Markewitz and JP Schmidt, for their constant encouragement and guidance throughout my time at UGA; without their help this thesis would not have been possible. I would also like to thank both Larry Morris and Bill Miller on my advisory committee for their help and input throughout the thesis process.

I would also like to thank the Natural Resources Conservation Service for their partial financial support with this project. I greatly appreciate the assistance of Daniel Wallace and Dee Pederson, as well as the Joseph W. Jones Ecological Research Center, John Traylor, and Mac Callahan for access to properties and help in the field.

I also want to thank my lab group, Karla Gann, Rachel Ryland, Jill Qi, Maryam Foroughi, Robert Brown, Lori Sutter, George Mathew, and Aaron Joslin, for their constructive criticism, help in the lab, and continued moral support throughout this processes. Finally, I must thank my family and friends outside of Warnell, as they have been a constant source of support and advice.

TABLE OF CONTENTS

LIST OF TABLES

Page

LIST OF FIGURES

Page

CHAPTER 1

INTRODUCTION

As interest in spatially explicit soil sampling has developed for both precision agriculture and ecological modeling, demands for rapidly acquired and more extensive soil quality data have increased (McBratney et al., 2006). Soil analyses are often restricted to relatively few samples or samples that are composited across an area to provide a representative mean, but such approaches lack the data richness to determine local or fine-scale spatial variability (Soriano-Disla et al., 2014). Visible/near-infrared reflectance (VNIR) spectroscopy is developing into a viable option to determine soil properties in the field in a more rapid, cost effective, and spatially explicit manner.

Many studies on VNIR-based models have investigated the effect of using different multivariate techniques and different spectral preprocessing methods on prediction accuracy. In addition to total soil C, studies have investigated SOC, clay content, and pH (Vasques et al., 2008; Rossel and Behrens, 2010). Working in north-central Florida, Vasques et al. (2008), used partial least square regression (PLSR) and other multivariate techniques with spectral preprocessing to predict total soil carbon and SOC. Vasques et al. (2008) determined that PLSR yielded the best prediction. In contrast, Rossel and Behrens (2010) using soil samples from Australia to predict SOC, pH, and clay content, compared PLSR and support vector machines (SVM), and other multivariate techniques combined with spectral preprocessing transformations. These

researchers found SVM to be the best algorithm for predicting all three soil properties. More recently, Curcio et al. (2013) found PLSR with the continuum removal (CR) transformations to best correlate specific spectral absorption features with soil texture properties. No consensus exists with respect to the best multivariate technique and spectral preprocessing for calibration across soil types and properties.

The longleaf pine (*Pinus palustris*) ecosystem of the southeastern US is an ecosystem of conservation concern and a focus of restoration efforts. During restoration, the recovery of SOC can reflect the development of organic matter and nutrient cycles in this ecosystem. As such, the ability to rapidly and spatially monitor SOC concentrations with VNIR would be valuable. This requires good VNIR calibrations of soil properties for soil series supported by longleaf pine.

Longleaf pine forests once encompassed more than 90 million acres across the southeast United States, stretching from eastern Texas to southern Virginia. Over the past two centuries, development, timber harvest, and fire suppression have reduced the extent of these forests by almost 97 percent (Longleaf Alliance, 2015). The species extensive historic range demonstrates its ability to thrive on a variety of soils within the Southeast, ranging from the xeric sandy Entisol soils of the Coastal Plain to the mesic clayey Ultisol soils of the Piedmont and the wet mesic Spodosols of the Flatwoods region (Mclntyre et. al. 2008; Peet 2006). Given the ecological breadth of longleaf pine, VNIR calibrations would need to be robust on multiple soil series. There are 296 soil series in the state of Georgia and more than half can support longleaf pine (Environmental Protection Division, 2000).

Regeneration and restoration of the longleaf pine ecosystem in these regions has become an important goal of many groups and government agencies including the Longleaf Alliance, National Fish and Wildlife Foundation, The Nature Conservancy, U.S. Forest Service, and the Natural Resource Conservation Service (NRCS). The NRCS, in particular, participated in the Conservation Reserve Program's Longleaf Pine Initiative (LLPI) that started in 2006 to plant marginal agricultural lands to longleaf pine and in 2010 the NRCS extended the LLPI to foster regeneration and restoration of longleaf pine on private lands (NRCS, 2011).

The historical range of the longleaf pine ecosystem has been designated a priority landscape by the NRCS and the agency has worked to develop a range of state-and-transition-models that identify expected transitions in ecological site conditions with a change in management (i.e., agricultural abandonment or introduction of fire). When considering restoration and regeneration of longleaf pine within this framework of state-transitions for a particular ecological site there is an interest in understanding how soil characteristics may vary with landscape position, and thus impact longleaf pine communities, and how changing management will change soil properties. The state-and-transition models are designed for specific physiographic settings and ecological site descriptions (ESD) that are predominantly defined by plant communities but also by soil properties (Caudle et al. 2013).

When studying dynamic soil properties (DSP; i.e., properties that are expected to change on human timescales of decades to centuries) such as pH or organic carbon, it is recommended that studies focus on specific soil map units, specifically the soil series

(Tugel et al., 2008). However, this recommendation does not address the fact a soil series is only one component of a map unit. Differences in slope, historic erosion or other features indicated by the map unit may be as, or more important, than the soil series itself for determining vegetation-soil relationships (Soil Survey Division Staff, 1993). As such, when studying DSPs under longleaf pine one might keep the soil series consistent while sampling across different map unit phases with varying slope, which can impact both longleaf pine communities and soil attributes. Currently, there is little research on how soil map units incorporating steepness of slope within a soil series might influence longleaf pine community classification or, more generally, how these differences might impact DSP under longleaf pine regeneration or restoration.

This thesis focuses on the use of visible/near-infrared scanning as a method to rapidly and cost effectively analyze and predict soil properties in the field, while also focusing on the use of soil map units as a useful attribute to analyze DSPs along topographic gradients within longleaf pine ecosystems. In Chapter II of this thesis, using soils under longleaf pine management, I produce a predictive model to determine soil total carbon by means of VNIR spectroscopy using a variety of spectral transformations and algorithms. In Chapter III I analyze adjoining soil map units that vary in slope steepness at four different sites, two located within the Piedmont region and two within the Middle Coastal Plain region of Georgia. I use VNIR in analyses of soil properties of interest (i.e., carbon, clay, and pH_{cacl2}) that may help evaluate soil variability topographically or DSPs over time and under changing land use. In Chapter IV I briefly discuss the overall importance of this thesis.

References

Caudle, D., Sanchez, H., DiBenedetto, J., Talbot, C., & Karl, M. S. (2013). *Interagency ecological site handbook for rangelands*. US Department of the Interior, Bureau of Land Management.

Curcio, D., Ciraolo, G., D'Asaro, F., & Minacapilli, M. (2013). Prediction of Soil Texture Distributions Using VNIR-SWIR Reflectance Spectroscopy. *Procedia Environmental Sciences, 19*: 494-503. doi: 10.1016/j.proenv.2013.06.056

Georgia Soil and Water Conservation Commission. (2000). Manual for erosion and sediment control in Georgia. *Atlanta, GA.*

Longleaf Alliance. (2015). *About Longleaf*. Retrieved from http://www.longleafalliance.org/

McBratney, A. B., Minasny, B., & Rossel, R. V. (2006). Spectral soil analysis and inference systems: a powerful combination for solving the soil data crisis. *Geoderma*, *136*(1): 272-278.

Mclyntyre, R.K; Jack, S.B; Mitchell, R.J.; Hiers, J. K.; Neel, W.L. (2008). Multiple Value Management: The Stoddard~ Neel Approach to Ecological Forestry In Longleaf Pine Plantations. *Joseph W. Jones Ecological Research Center*. Retrieved from http://www.americaslongleaf.org/media/3536/multiple_value_management_the_stoddard-neel_approach_to_ecological_forestry.pdf

Natural Resource Conservation Service (NRCS). (2011). *Longleaf Pine Initiative.* Retrieved from http://www.nrcs.usda.gov/wps/portal/nrcs/detailfull/national/home/?cid=nrcsdev11_023913.

Peet, R. K. (2006). Ecological classification of longleaf pine woodlands. In *The Longleaf Pine Ecosystem* (pp. 51-93). Springer New York.

Rossel, R. A. V., & Behrens, T. (2010). Using data mining to model and interpret soil diffuse reflectance spectra. *Geoderma, 158*(1-2): 46-54. doi: 10.1016/j.geoderma.2009.12.025

Soil Survey Division Staff. (1993). Soil survey manual. Soil Conservation Service. U.S. Department of Agriculture Handbook 18.

Soriano-Disla, J. M. , Janik, L. J., Rossel, R. A. V., Macdonald, L. M., & McLaughlin, M. J. (2014) The Performance of Visible, Near-, and Mid-Infrared Reflectance Spectroscopy for Prediction of Soil Physical, Chemical, and Biological Properties, *Applied Spectroscopy Reviews*, 49(2): 139-186, DOI: 10.1080/05704928.2013.811081

Tugel, A. J., Wills, S. A., and Herrick, J. E. (2008). Soil Change Guide: Procedures for Soil Survey and Resource Inventory, Version 1.1. USDA, Natural Resources Conservation Service, National Soil Survey Center, Lincoln, NE.

Vasques, G.M., Grunwald, S. & Sickman, J.O. (2008). Comparison of multivariate methods for inferential modeling of soil carbon using visible/near-infrared spectra. *Geoderma 146*(1-2): 14–25. doi:10.1016/j.geoderma.2008.04.007

CHAPTER II

VNIR CALIBRATIONS FOR SOIL TOTAL CARBON ACROSS SOIL SERIES UNDER LONGLEAF PINE ECOSYSTEMS[1]

[1]Stockton, J.C. and Markewitz, D. 2016. To be submitted to *Communications in Soil Science and Plant Analysis*

Abstract

Visible/near-infrared reflectance (VNIR) spectroscopy has been shown to be an extremely flexible method for the rapid analysis of many soil properties. VNIR scans of samples collected from a range of soil series under longleaf pine (*Pinus palustris*) were calibrated with soil total carbon using different multivariate methods to assess measurement accuracy. Spectra were preprocessed using three different transformation methods; Savitzky-Golay, continuum removal, and wavelets. Two multivariate algorithms, the partial least square regression (PLSR) and support vector machine (SVM), were used to determine the best calibration model based on the coefficient of determination (R^2) and root mean square error (RMSE) on training and test data sets. Most samples included in this dataset were procured through the Rapid Carbon Assessment (RaCA) database from the Natural Resources Conservation Service (NRCS) where 900 samples contained both VNIR scans and soil total carbon values. Data were analyzed for three data subsets; all soils, organic matter horizons with 17 - 60 % C values, and mineral soil with 0-2% C values. Results indicate that the SVM algorithm combined with the SG transformation provides the best calibration and validation prediction of R^2=0.70 for mineral soils. Mineral soils also produced the lowest RMSE compared to all other levels of analysis. VNIR offers a cost effective and rapid means for capturing soil total carbon in the field to evaluate management and restoration effects on soils in longleaf pine ecosystems.

Introduction

As interest in spatially-explicit soil sampling has developed for both precision agriculture and ecological modeling, demands for rapidly acquired and more extensive soil quality data have increased (McBratney et al., 2006). Soil analyses are often restricted to relatively few samples or samples that are composited across an area to provide a representative mean, but such approaches lack the data richness to determine local or fine-scale spatial variability (Soriano-Disla et al., 2013). Visible/near-infrared reflectance (VNIR) spectroscopy is developing into a viable option to determine soil properties in the field in a more rapid, cost effective, and spatially explicit manner that can expand the acquisition of soil data.

In VNIR scanning, spectral reflectance is measured from soils across a range of spectral wavelengths (350 – 2500 nm) that include both visible and a portion of infrared wavelengths. Spectral reflectance measures the ratio of radiant energy reflected from a surface to that incident on the surface, it can be increased or decreased by factors such as soil moisture, organic matter content, soil texture, and mineralogy (Lillesand et al., 2008). Through the use of VNIR reflectance spectroscopy and known soil properties values, statistical models can be developed to predict soil properties within the laboratory and field.

Many studies on VNIR-based models have investigated the effect of using different multivariate techniques and different spectral preprocessing methods on prediction accuracy. In addition to total soil C, studies have also investigated other properties such as SOC, clay content, and pH (Vasques et al., 2008; Rossel and Behrens, 2010). Working

in north-central Florida, Vasques et al. (2008), used partial least square regression (PLSR) and other multivariate techniques with spectral preprocessing to predict total soil carbon and SOC. Vasques et al. (2008) determined that PLSR yielded the best prediction. In contrast, Rossel and Behrens (2010) using soil samples from Australia to predict SOC, pH, and clay content, compared PLSR and support vector machines (SVM), and other multivariate techniques combined with spectral preprocessing transformations. These researchers found SVM to be the best algorithm for predicting these three soil properties. More recently, Curcio et al. (2013) found PLSR with the continuum removal (CR) transformations to best correlate specific spectral absorption features with soil texture properties. Inconsistencies in the literature reveal that no consensus exists with respect to the best multivariate technique and spectral preprocessing for calibration across soil types and properties.

Longleaf pine (*Pinus palustris*) is an ecosystem of conservation concern and thus a focus of restoration efforts. During restoration, the recovery of SOC can reflect the development of organic matter and nutrient cycles in this ecosystem. The ability to rapidly and spatially monitor SOC concentrations with VNIR would be valuable for documenting restoration success. Longleaf pine has the ability to live and thrive on a variety of soils within the southeast United States, ranging from the sandy soils of the Coastal Plain to clayey soils in the Piedmont (Mclntyre et. al. 2008). Historically, longleaf pine covered most of the Atlantic and Gulf Coastal Plains from southeastern Virginia to eastern Texas and south through the northern two-thirds of peninsular Florida, an area of approximately 90 million acres. Currently, due to timber harvesting, clearing

for agriculture, and suburban development, the longleaf pine ecosystem has dwindled to approximately 3.8 million acres, mainly in northern North Carolina, eastern Louisiana, and Florida (Figure 2.1; Longleaf Alliance, 2015). Given the ecological breadth of longleaf pine, VNIR calibrations will need to be robust across multiple soil series. For example, there are 296 soil series in the state of Georgia and more than half can support longleaf pine (Environmental Protection Division, 2000).

Loss of longleaf pine has decreased habitat for many endemic plants and led some animal species to become endangered. Wiregrass (*Aristida stricta)*, the purple pitcher plant (*Sarracenia purpurea),* the red-cockaded woodpecker (*Leuconotopicus borealis*), and the gopher tortoise (*Gopherus Polyphemus)* are species that depend on the longleaf pine ecosystem.

The diversity and historical range of the longleaf pine ecosystem is intertwined with its fire history. Longleaf pine is a prime example of a fire-dependent ecosystem. Without fire, deciduous tree species invade, and their shade eliminates both the longleaf pine regeneration and herbaceous understory vegetation (Mississippi Forestry Commission, 2008). Historically, lightning ignited fires that burned across the landscape did not cause catastrophic damage. More recently, due to fire suppression, which leads to the buildup of fuels, fires have burned with greater intensity (Wilson et al., 2002). Prescribed fires can ameliorate these fuel conditions and accomplish a number of additional objectives including preparing sites for seeding and planting, improving wildlife habitat, managing competing vegetation, controlling insects and disease, improving forage for grazing, enhancing aesthetics, and providing a foothold for a

diversity of understory vegetation (Kavanagh et al. 2010). The use of prescribed fire within longleaf pine ecosystems has been central to restoring and regenerating this species across its native range. Unfortunately, in addition to the need to calibrate across many soil series, fire may further complicate VNIR calibrations as it would be very difficult to incorporate a metric of time since last fire or intensity of fire at a specific location into calibrations. However, robust predictions of total soil C across this range of variance within the longleaf pine ecosystem may help to better inform future restoration and regeneration management.

Therefore, the primary aim of this study is to identify the best multivariate techniques and spectral transformations for soils under longleaf pine ecosystems. PLSR and SVM are compared and the coefficient of determination (R^2) is used as the goodness-of-fit metric to find the best approach for predicting soil total carbon in these soils. PLSR and SVM, both widely used in chemometrics (Marabel et al. 2013), use the entire spectrum of available data. Three preprocessing transformations are also compared with each multivariate technique, Savitzky-Golay (SG), continuum removal (CR), and wavelets (WT). These six combinations are compared for the best prediction of total soil carbon in longleaf pine soils.

With the development of accurate predictive models, soil total carbon values can be measured by scanning a soil sample either *in situ* or in a laboratory. Given non-linear relationships between VNIR reflectance and soil properties, it is predicted that SVM will provide a better model than PLSR (Thissen et al., 2004; Üstün, 2003).

Methods

Dataset

Data used in this study were acquired through the Rapid Carbon Assessment (RaCA) (n=346) conducted by the Natural Resources Conservation Service (NRCS). A secondary set of data, not included in the RaCA database, were provided by Strickland et al. (2015) (n=585). The complete national RaCA database encompasses over 6,000 samples across the United States. From these, 346 data entries were extracted from the RaCA database by soil series found under the longleaf pine historical range. These 346 data entries consist of both carbon measurements and VNIR scans within the soil profile. Both scans and carbon values were collected using a range of techniques through different laboratories participating in the RaCA database project. The Strickland et al. (2015) samples (n=585) consist of only carbon measurements. These soil samples were provided to us by Dr. Strickland so that VNIR scanning could be completed. The total dataset within this study (n = 909) includes 22 different soil series in 284 profiles (Table 2.1). Not all soil profiles were sampled according to the same depth increments or data collection techniques. Total profile depth within the dataset ranged from 0 - 65 cm to 0 - 305 cm, and depth increments varied by profile. Carbon values ranged from 0.01 to 59.84 % (Figure 2.2a).

Laboratory Methods

A VNIR field Spectrophotometer (Analytical Spectral Devices, Boulder, Co.) with Indico Pro software and a contact probe with a window diameter of 2 cm was used

to scan soil samples from Strickland et al. (2015) from 350 to 2500 nm in 1 nm increments. A baseline scan using a Spectralite® white blank (ASD, Inc.) was preformed to initiate measurements. After establishing the base line, the contact probe lens was pressed firmly against the surface of a soil sample within its sample bag so that no light from the lens was visible and then scanned. The soil was then mixed within the sample bag, and a refreshed surface was scanned again. Each spectrum was averaged from a compilation of 50 readings during each scan. Three scans per sample were performed, which were then averaged. Between each sample, the contact probe was cleaned. A baseline scan was performed after every 10 samples.

Calibration Process

Raw reflectance spectra were preprocessed by cleaning and smoothing in R version 3.2.3 by using Savitzky-Golay (SG), continuum removal (CR), or wavelets (WT) transformations within the prospectr and soil.spec packages (Sila et al., 2014; Stevens et al. 2013). Transformations of these data were done to reduce the dimensionality of the spectral data, which can improve the prediction of the calibrations. The SG uses the first derivative of the spectra across an eleven band window (Savitzky & Golay, 1964). The CR finds points lying on the convex hull (local maxima or envelope) of a spectrum, connects the points by linear or spline interpolation and normalizes the spectrum by dividing (or subtracting) the input data by the interpolated line (Stevens et al. 2013). The WT is an integral transformation that smooths spectral signals and reduces the dimensionality of large data sets (Rossel et al., 2009; Szu et al., 1996). Low signal to

noise ranges were removed (350-380, 970-1010, and 2460-2500 nm) after transformations were completed (Shepherd et al., 2002).

Spectra and carbon data were randomly separated into 20% test and 80% training datasets. To avoid splitting up soil profiles, the Kennard-Stone Algorithm was used (Kennard & Stone, 1969). The PLSR or SVM was used to perform the calibration (Figure 3). The PLSR is a linear predictive algorithm, whereas SVM is a linear algorithm but in a high-dimensional space. SVM performs classification tasks by forming an optimal separating hyperplane between two classes by maximizing the margin between the classes' closest points. Points lying on the boundaries are called support vectors, and the middle of the margin is the optimal separating hyperplane (Meyor et al., 2015; Thissen et al., 2004; Üstün, 2003).

Coefficients of determination (R^2) were determined for the training dataset along with a cross-validation. During the cross-validation the training datasets were partitioned into 10 random folds and trained over nine folds while being validated on the 10th. This was repeated nine times for each of the folds and the accuracy averaged over all of them. In addition, R^2 was determined for a linear regression on the observed vs predicted values in the test datasets along with the root mean square error (RMSE) where

$$RMSE = \sqrt{\frac{1}{n}\sum_{i=1}^{n}(yi - y\hat{i})^2}$$

n is the number of samples, yi is the measured carbon value, and $y\hat{i}$ is the predicted carbon value.

Calibration Data

In order to determine the best calibration, the data was analyzed in three groupings*:* (1) calibrations of all data available (All soil, n = 931); (2) calibration of O horizon data only, in which C values ranged from 17.69 – 59.84% and were squared to achieve statistical normality (O horizon, n =227) (Figure 2.2b); and (3) calibrations on mineral soil data only containing C values from 0.01 - 2% for which we used a log10 transformation to achieve normality (mineral soil, n = 682) (Figure 2.2c).

Results

For the training/cross-validation data, the All Soil analysis found that PLSR with CR yielded R^2 = 0.94 compared to 0.95 and 0.95 for SG and WT transformations (Table 2.2). In contrast, SVM with CR, SG, and WT yielded R^2 =0.96, compared to 0.96 and 0.96 for SG and WT. For Organic Horizon data, PLSR with CR yielded R^2 = 0.74 compared to 0.99 and 0.93 for SG and WT. SVM produced much poorer fits, yielding R^2 = 0.56, 0.58, and 0.53 for CR, SG, and WT. For the Mineral Soil analysis, PLSR with CR yielded R^2 = 0.79 compared to 0.86 and 0.81 for SG and WT, and SVM yielded R^2 = 0.79, 0.86 and 0.85 for CR, SG, and WT. Mineral soil analysis resulted mostly in lower *RMSE* fits than either All Soil or the O Horizon analyses (Table 2.2).

Using these multivariate models total soil carbon was predicted for the test dataset and predicted values compared with observed. For All Soil analysis, PLSR with CR yielded R^2 = 0.77 on test/validation data compared to 0.80 and 0.80 for SG and WT transformations. In contrast, SVM with CR yielded R^2 =0.78, compared to 0.80 and 0.69

for SG and WT (Figure 2.4). For Organic horizon data, PLSR with CR yielded R^2 = 0.36 on validation data compared to 0.23 and 0.23 for SG and WT (Figure 2.5). SVM produced much better fits, yielding R^2 = 0.38, 0.45, and 0.39 for CR, SG, and WT (Figure 2.5). For the mineral soil analysis, PLSR with CR yielded R^2 = 0.64 on validation data compared to 0.64 and 0.64 for SG and WT, and SVM yielded R^2 = 0.61, 0.70 and 0.70 for CR, SG, and WT (Figure 2.6). Mineral soil analysis also resulted in lower *RMSE* than either All Soil or the Organic Horizon analyses (Table 2.2).

Discussion

The All Soil analysis results yielded the best validation and cross-validation as measured by R^2 with the PLSR and WT combination producing the best model (Table 2). However, the combination of organic and mineral soil horizons forms a bimodal distribution of total C (Figure 2.2a) and the validation plots (Figure 2.4) indicate soil total C percentages span a large range (0.01 – 59.84%), but with most samples located at each extreme. Due to this bimodal distribution, cross-validation and validation results are problematic and dictate the use of separate calibrations for organic vs. mineral horizons.

The SVM model with the SG transformation performed best for the Organic horizon data, which contain the higher C values. This model had a cross-validation R^2 of 0.64 and a validation R^2 of 0.55. This relatively low cross-validation result indicates that the model is somewhat ineffective as predictions using data from within the training dataset should generally be quite good (i.e., R^2>0.9). These low R^2 values within the Organic horizon level may be due to the high organic matter contents. Generally,

spectrophotometric techniques can produce asymptotic shaped response curves as at high concentrations each increment of carbon no longer produces a linear response. At the extreme, the response to additional C maybe so flat that concentrations cannot be separated. This could partly explain the calibration's inability to predict soil total C within the Organic horizon.

The Mineral soils (0.01 - 2% C) calibration using SVM and SG yielded the most accurate prediction (R^2 = 0.86 on cross-validation and R^2 = 0.70 on validation). Moreover, from the plot's well-distributed residuals this calibration appears superior to all others (Figure 2.2c). While a predictive performance of R^2 = 0.70 is still too low for accurate measurement of soil total carbon, this particular model might still assist in inferring horizontal spatial variance or vertical variance. These results suggest that the RaCA dataset as a whole may be too broad in soil series, landscape type, and soil total C ranges, with insufficient replication within these groups, to be fully able to accurately predict soil total C across a diverse region such as the longleaf pine ecosystem.

Similar calibration difficulties were found by Stenberg (2010) working with a dataset (n = 396) representative of agricultural soils in Sweden. The 396 samples were organized into 5 categories of sand percentages (0-20, 20-40, 40-60, 60-80 and 80-100% sand) with grain sizes ranging between 0.06 and 2.0 mm in diameter. Stenberg was able to determine an effective calibration model for SOC only when sandy soils (80-100 % sand) were removed from the dataset. Homogenizing the soil types resulted in lower RMSE on average (ranging from ~ 0.625-0.71) than when removing other categories of sand. Within the current study, texture was not available, making it possible that texture

(i.e. the percentage of sand) could be another variable affecting the model. A number of studies (Wang et al. 2015; Soriano-Disla et al. 2014, Sá et al. 2009; Vasques et al. 2008) achieved favorable calibrations ($R^2 > 0.8$) on homogenous soil data sets. For example, Wang et al. (2015) sampled 675 soil samples within Nebraska, California and Texas agriculture fields collected at three depths (0-15, 15-30, 30-45 cm). For soil total C, the study produced R^2 between 0.84-0.87 for each field. These studies that achieved favorable calibrations possibly within more homogenous soils suggests NIRS calibration may not be broadly applicable across multiple soil series.

Generally, SVM yielded better (smaller) RMSE validation statistics than PLSR, across transformations and data groups. Based on both higher validation R^2 and smaller RMSE values, regardless of transformation used, SVM proved to be a more accurate and flexible model for predicting total soil C than PLSR.

In the future, VNIR calibration models may benefit from including more variables into the calibration equation, such as land use type and depth of sample. The dataset used in this study derives from a mixture of sampling depths, sampling methods, C analysis methods, and land use types. By incorporating different land uses and different depth measurements into the calibration, it may be possible to construct a total soil C calibration with greater accuracy.

Conclusion

Results support the hypothesis that SVM performs better than the more-constrained PLSR. While SVM combined with SG for 0 -2 % C (mineral soil) yielded

the highest prediction accuracy (R^2 = 0.70) it is not yet equipped to be used as a prediction model for soil total C with sufficient accuracy. Across such a diverse ecosystem as the longleaf pine ecosystem a more robust calibration will be required. This lack of precision, in part, may be due to the high degree of spatial variability within the dataset and data collection inconsistencies. However, where spatial patterns are concerned, this model could do well in trying to provide some inference for horizontal or vertical spatial variance.

References

Curcio, D., Ciraolo, G., D'Asaro, F., & Minacapilli, M. (2013). Prediction of Soil Texture Distributions Using VNIR-SWIR Reflectance Spectroscopy. *Procedia Environmental Sciences, 19*: 494-503. doi: 10.1016/j.proenv.2013.06.056

Georgia Soil and Water Conservation Commission. (2000). Manual for erosion and sediment control in Georgia. *Atlanta, GA.*

Kavanagh, K., Koyama, A., & Stephan, K. (2010). After the Fire, Follow the Nitrogen. Retrieved December 1, 2015, from https://www.firescience.gov/projects/briefs/04-2-1-97_FSBrief92.pdf

Kennard, R. W., & Stone, L. A. (1969). Computer aided design of experiments. *Technometrics, 11*(1): 137-148.

Lillesand, Kiefer, & Chipman. (2008). *Remote Sensing & Image Interpretation*. (6th ed.). Hoboken, NJ: John Wiley & Sons.

Longleaf Alliance. (2015). *About Longleaf*. Retrieved from http://www.longleafalliance.org/

Marabel, M. & Alvarez-Taboada, F. (2013). Spectroscopic Determination of Aboveground Biomass in Grasslands Using Spectral Transformations, Support Vector Machine and Partial Least Squares Regression. *Sensors, 13*: 10027-10051. doi: 10.3390/s130810027

McBratney, A. B., Minasny, B., & Rossel, R. V. (2006). Spectral soil analysis and inference systems: a powerful combination for solving the soil data crisis. *Geoderma, 136*(1): 272-278.

Mclyntyre, R.K; Jack, S.B; Mitchell, R.J.; Hiers, J. K.; Neel, W.L. (2008). Multiple Value Management: The Stoddard~ Neel Approach to Ecological Forestry In Longleaf Pine Plantations. *Joseph W. Jones Ecological Research Center.* Retrieved from *ht*tp://www.americaslongleaf.org/media/3536/multiple_value_management_the_stoddard-neel_approach_to_ecological_forestry.pdf

Meyer, D.; Hornik, K; Dimitriadou, E.; Weingessel, A.; Leisch, F. (2015). e1071: Misc Functions of the Department of Statistics, Probability Theory Group (Formerly: E1071), TU Wien. R package version 1.6-7. https://CRAN.R-project.org/package=e1071

Mississippi Forestry Commission (2008). Benefits of Prescribed Fire Longleaf Pine. Retrieved December 3, 2015, from http://www.mfc.ms.gov/pdf/Pubs/Benefits_Prescribed_Burning_LL_Pines.pdf

Reeves, J. B. (2010). Near- versus mid-infrared diffuse reflectance spectroscopy for soil analysis emphasizing carbon and laboratory versus on-site analysis: Where are we and what needs to be done? *Geoderma*, *158*(1-2): 3-14. doi: 10.1016/j.geoderma.2009.04.005

Rossel, R. A. V., & Behrens, T. (2010). Using data mining to model and interpret soil diffuse reflectance spectra. *Geoderma*, *158*(1-2): 46-54. doi: 10.1016/j.geoderma.2009.12.025

Rossel, R. A. V., & Lark, R. M. (2009). Improved analysis and modelling of soil diffuse reflectance spectra using wavelets. *European Journal of Soil Science*, *60*(3): 453-464.

Sá, S. O., Althmann, D., Figueiredo, K. L., Bernoux, M., Poppi, R. J., & Cerri, C. C. (2009). NIRS-LS-SVM to estimate carbon content of agricultural land in Brazilian Cerrado soils. IOP Conference Series: *Earth & Environmental Science*, 6(24): 2037. doi:10.1088/1755-1307/6/24/242037.

Savitzky, A., & Golay, M. J. (1964). Smoothing and differentiation of data by simplified least squares procedures. *Analytical Chemistry*, *36*(8): 1627-1639.

Shepherd, K. D., & Walsh, M. G. (2002). Development of reflectance spectral libraries for characterization of soil properties. *Soil Science Society of America Journal*, *66*(3): 988-998.

Sila A., Hengl, T., and Terhoeven-Urselmans, T. (2014). soil.spec: Soil Spectroscopy Tools and Reference Models. R package version 2.1.4.

Soriano-Disla, J. M. , Janik, L. J., Rossel, R. A. V., Macdonald, L. M., & McLaughlin, M. J. (2014) The Performance of Visible, Near-, and Mid-Infrared Reflectance Spectroscopy for Prediction of Soil Physical, Chemical, and Biological Properties, *Applied Spectroscopy Reviews*, 49(2): 139-186, DOI: 10.1080/05704928.2013.811081

Stenberg, B. (2010) Effects of soil pretreatments and standardized rewetting as interacted with sand classes on Vis-NIR predictions of clay and soil organic carbon. *Geoderma, 158:* 163-215.

Stevens, A. & Ramirez-Lopez, L. (2013). An Introduction to the Prospectr Package. R Package Vignette R Package Version 0.1.3.

Strickland, T. C., Scully, B. T., Hubbard, R. K., Sullivan, D. G., Abdo, Z., Savabi, M. R., & Hawkins, G. L. 2015. Effect of conservation practices on soil carbon and nitrogen accretion and crop yield in a corn production system in the southeastern coastal plain, United States. *Journal of Soil and Water Conservation*, 70(3): 170-181. doi:10.2489/jswc.70.3.170.

Szu, H., Telfer, B., & Garcia, J. (1996). Wavelet transforms and neural networks for compression and recognition. *Neural networks*, *9*(4): 695-708

Thissen, U., Pepers, M., Üstün, B., Melssen, W. J., & Buydens, L. M. C. (2004). Comparing support vector machines to PLS for spectral regression applications. *Chemometrics and Intelligent Laboratory Systems*, *73*(2): 169-179.

Üstün, B. (2003). A Comparison of Support Vector Machines and Partial Least Squares regression on spectral data. *Katholieke Universiteit Nijmegen*. Retrieved from: http://www.ru.nl/science/analyticalchemistry

Vasques, G.M., Grunwald, S. & Sickman, J.O. (2008). Comparison of multivariate methods for inferential modeling of soil carbon using visible/near-infrared spectra. *Geoderma 146*(1-2): 14–25. doi:10.1016/j.geoderma.2008.04.007

Wang, D., Chakraborty, S., Weindorf, D. C., Li, B., Sharma, A., Paul, S., & Ali, M. N. (2015). Synthesized use of VisNIR DRS and PXRF for soil characterization: Total carbon and total nitrogen. *Geoderma*, 243(244): 157-167. doi:10.1016/j.geoderma.2014.12.011

Wilson, C. A., Mitchell, R. J., Boring, L. R., & Hendricks, J. J. (2002). Soil nitrogen dynamics in a fire-maintained forest ecosystem: results over a 3-year burn interval. *Soil Biology and Biochemistry*, *34*(5): 679-689.

Table 2.1: The twenty-two soil series and their frequency within the dataset. Note that profiles are not all the same depth with some containing only one horizon.

	SOILSERIES NAME	NO. OF PROFILES
1	Tifton	75
2	Pungo	50
3	Leon	30
4	Rains	29
5	Pelham	24
6	Alapaha	15
7	Carnegie	11
8	Johnston	10
9	Chewacla	8
10	Byars	5
11	Troup	5
12	Goldsboro	4
13	Pinebarren	3
14	Lakeland	2
15	Norfolk	2
16	Ruston	2
17	Atmore	1
18	Dothan	1
19	Johns	1
20	Lexington	1
21	Linker	1
22	Noboco	1

Table 2.2: Prediction results of validation and cross-validation *RMSE* and R^2 for each data separation, method, and transformation combinations for prediction of total soil C. Methods: partial least square regression (PLSR) and support vector machine (SVM). Transformations: continuum removal (CR), Savitzky-Golay (SG), and wavelet (WT). N-comp is principle components utilized.

DATA GROUP	METHOD	TRANSFORMATION	N-COMP	VALIDATION		CROSS-VALIDATION	
				R^2	*RMSE*	R^2	*RMSE*
ALL SOIL (N=909)	PLSR	CR	5	0.77	1.1416	0.94	1.2335
		SG	7	0.80	1.1646	0.95	0.8859
		WT	20	0.80	0.8195	0.95	0.9361
	SVM	CR		0.78	1.1974	0.96	1.2252
		SG		0.80	1.0672	0.96	0.8874
		WT		0.69	0.6931	0.96	0.9371
ORGANIC HORIZON (N=227)	PLSR	CR	14	0.36	2293	0.74	2349
		SG	7	0.23	2377	0.99	2390
		WT	7	0.23	2426	0.93	2387
	SVM	CR		0.38	2314	0.56	2312
		SG		0.45	2339	0.58	2371
		WT		0.39	2367	0.53	2372
MINERAL SOIL (N=682)	PLSR	CR	11	0.64	1.5499	0.79	1.3502
		SG	12	0.64	0.6632	0.86	0.5012
		WT	11	0.64	0.6759	0.81	0.4866
	SVM	CR		0.61	1.4824	0.79	1.3454
		SG		0.70	0.5931	0.86	0.4946
		WT		0.70	0.6211	0.85	0.4864

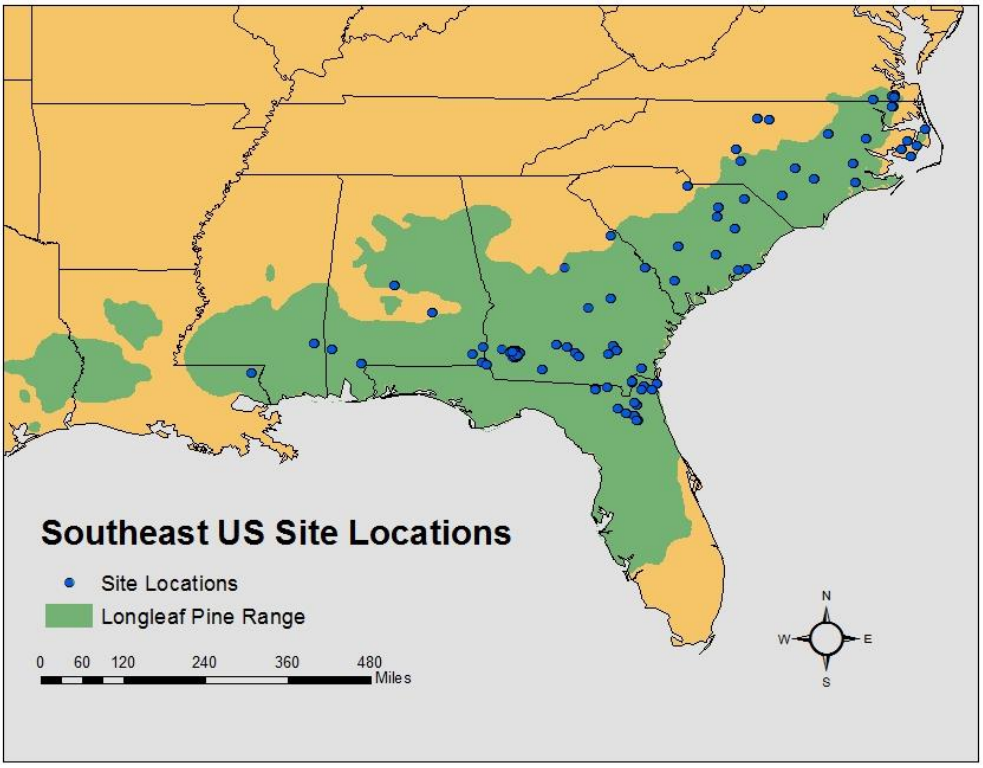

Figure 2.1: All site locations utilized for VNIR calibrations within the Southeastern U.S. shown over the native range of longleaf pine (green shading).

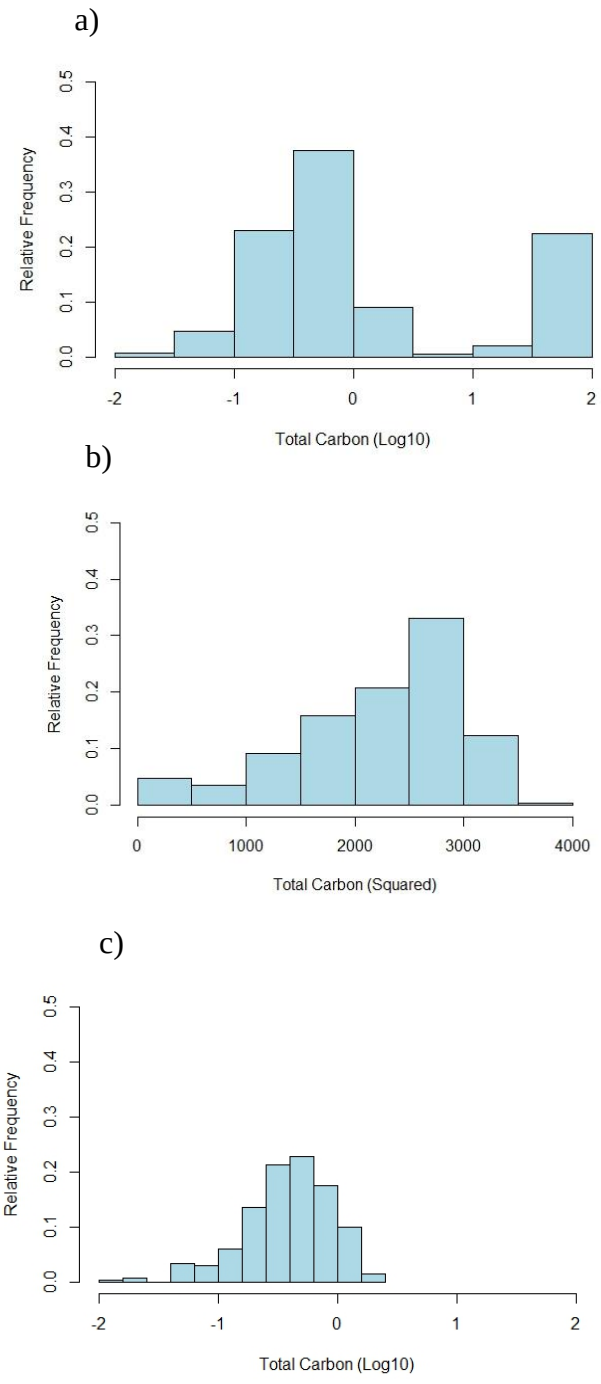

Figure 2.2: Relative frequency of soil total C for a) all data available, b) O Horizon data, and c) Mineral Soil data throughout sites located within the longleaf pine region in the southeast United States. Soil depth ranges to 2 m.

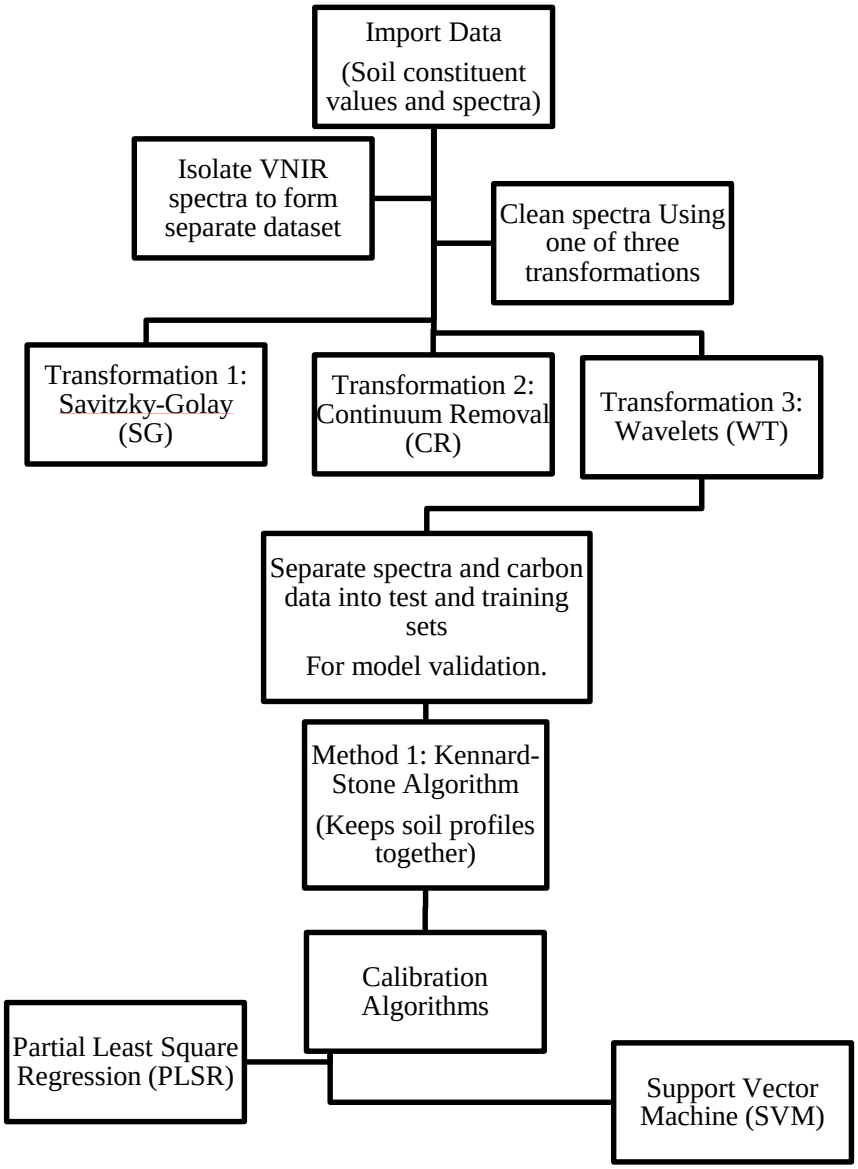

Figure 2.3: Flow chart describing multistep calibration process: (1) attribute data and spectra are collected, and spectra are cleaned; (2) spectral transformations are applied; (3) data are split into a training and test sets using the Kennard-Stone algorithm; (4) calibrations are developed on training and test sets using PLSR and SVM; and (5) calibrations are validated on the test set.

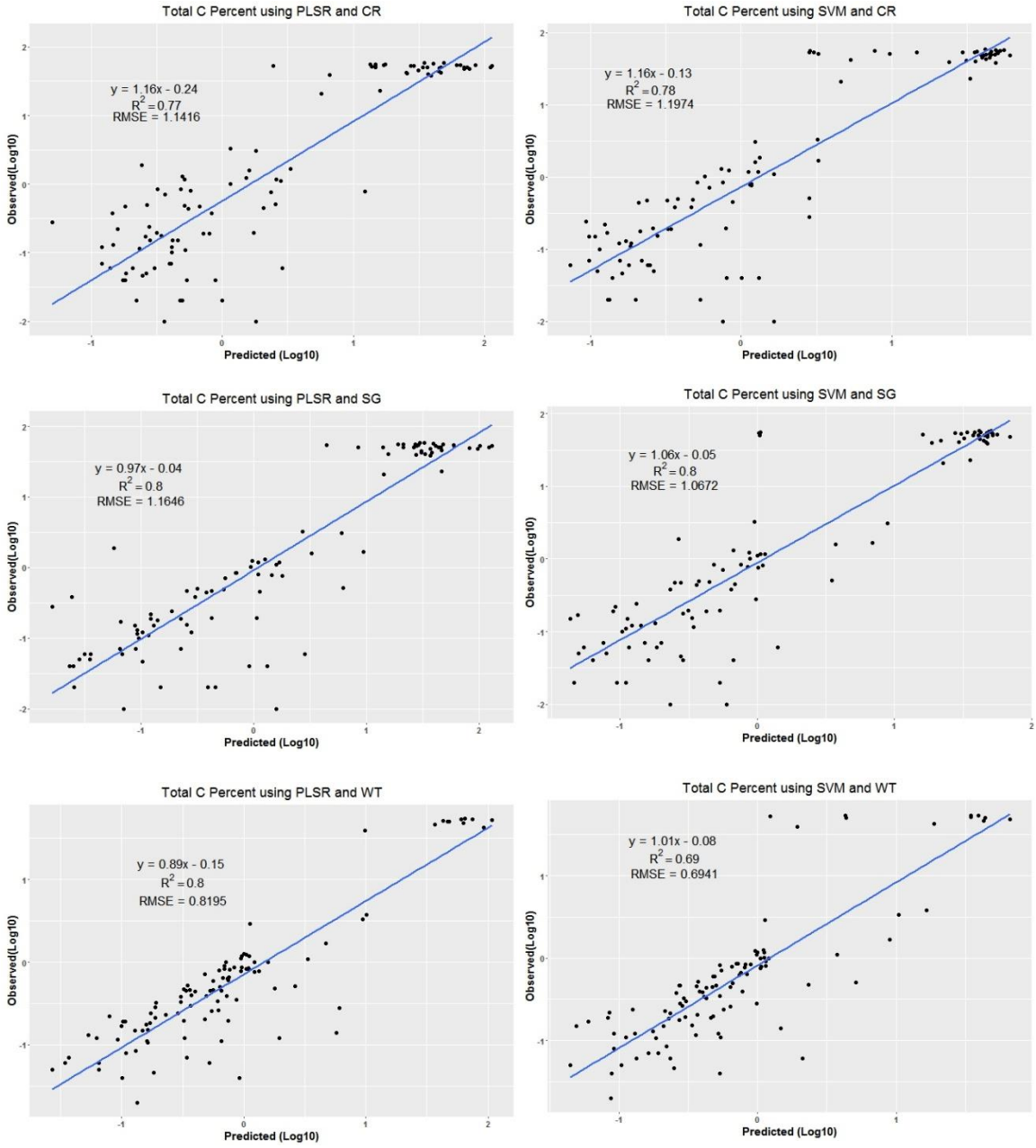

Figure 2.4: Validation scatter plot of total soil C measured vs. predicted soil C by partial least square regression (PLSR) and support vector machine (SVM) with continuum removal (CR), Savitzky-Golay (SG), or wavelet (WT) transformation using All Soil data collected under longleaf pine ecosystems.

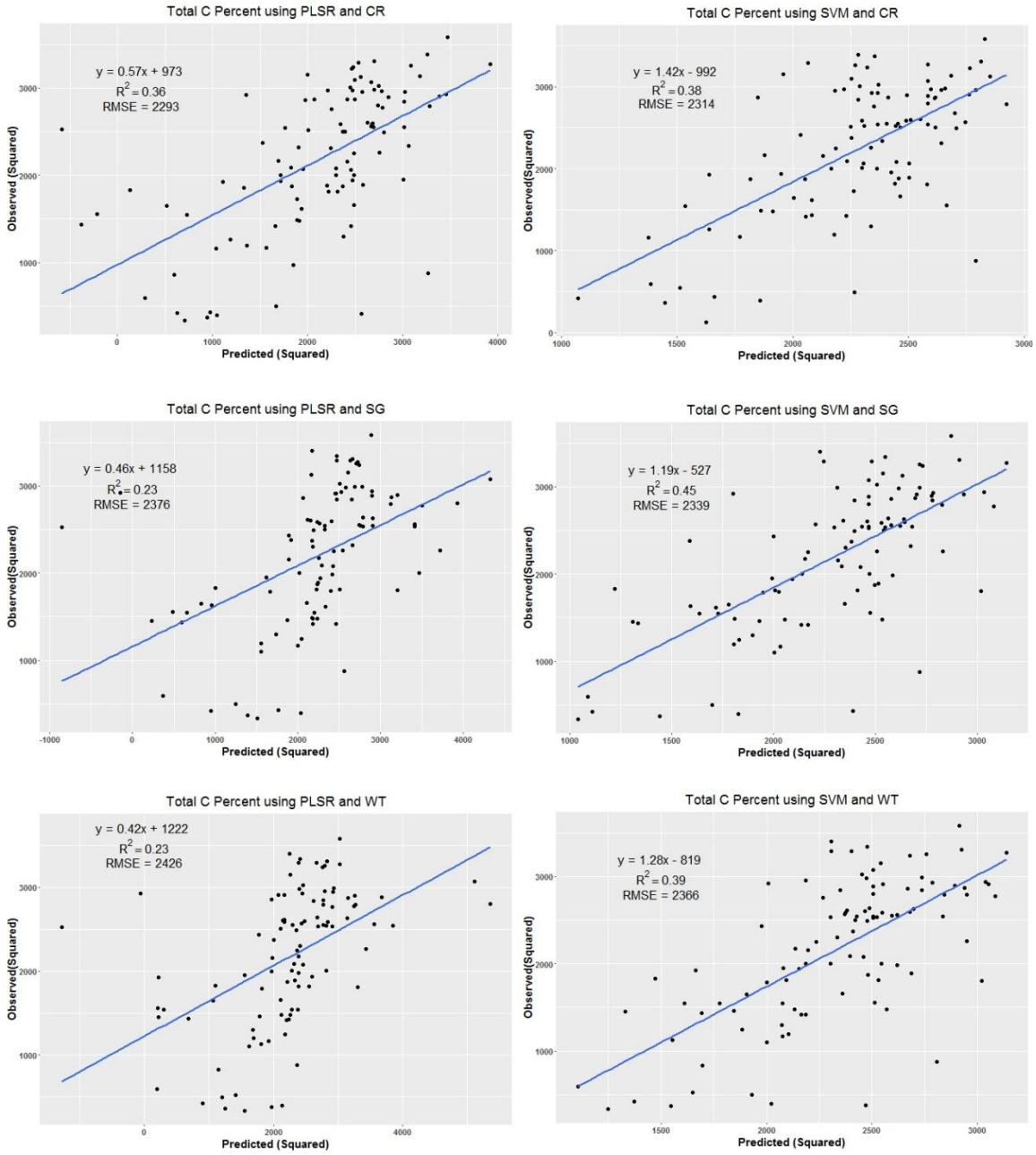

Figure 2.5: Validation scatter plot of total soil C measured vs. predicted by partial least square regression (PLSR) and support vector machine (SVM) with continuum removal (CR), Savitzky-Golay (SG), or wavelet (WT) transformation using O Horizon (17.69- 59.84% C) data collected under longleaf pine ecosystems.

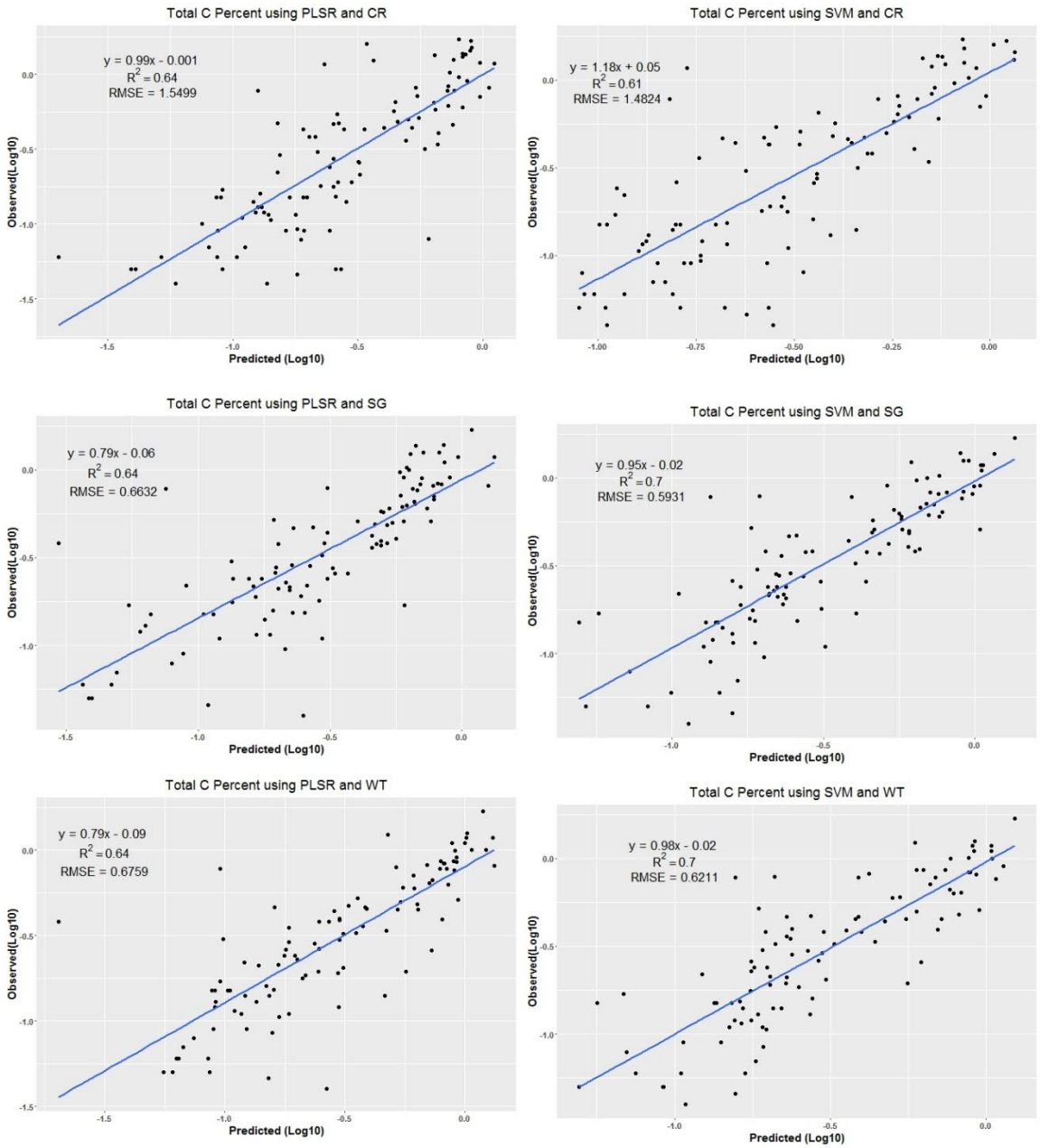

Figure 2.6: Validation scatter plot of total soil C measured vs. predicted by partial least square regression (PLSR) and support vector machine (SVM) with continuum removal (CR), Savitzky-Golay (SG), or wavelet (WT) transformation for mineral soil (0-2% C) data collected under longleaf pine ecosystems.

CHAPTER III

ANALYSIS OF SOIL MAP UNITS ACROSS SLOPE STEEPNESS WITHIN LONGLEAF PINE ECOSYSTEMS [1]

[1]Stockton, J.C. and Markewitz, D. 2016. To be submitted to *Geoderma Regional.*

Abstract

This study evaluated whether adjoining soil map units that vary in slope have sufficiently varying soil property profiles to impact analyses of soil change under longleaf pine management. Four different sites were sampled, one located within the Piedmont region, one within the Upper Coastal Plain region and two within the Middle Coastal Plain region of Georgia. All sites were dominated by an overstory of longleaf pine. A total of 24 profiles were collected to a depth of 0 – 200 cm with each site containing two or three map units and two or three profiles within each map unit. This study also incorporated the use of visible/near-infrared (VNIR) spectroscopy as a rapid, field based approach for analyzing soil properties of interest (i.e., clay, carbon, and pH_{cacl2}) that can aid in quantifying soil variability across topographic gradients or dynamic soil properties (DSP) over time. Results indicate that soil map unit phases capturing steepness of slope is not a valuable stratification variable in analyzing DSP under longleaf pine regeneration or restoration. Few significant differences were observed with slope steepness at any depth (0-200 cm) for the soil properties measured (percent clay, percent C, pH). Values of the soil properties measured ranged broadly across the sites and between depths. Percent clay ranged from less than 1 to greater than 70%, percent carbon ranged from 0 to 2.64%, and pH ranged from 3.42 to 6.17. VNIR calibrations for percent clay demonstrated potential predictive value (i.e., $R^2 \geq 0.9$) while those for C and pH_{cacl2}, though much lower (i.e., $R^2 \geq 0.67$ and $R^2 \geq 0.54$, respectively), indicated some utility for field classification or monitoring of DSP under longleaf pine ecosystems.

Introduction

Longleaf pine (*Pinus palustris*) forests once encompassed more than 90 million acres across the southeastern United States, stretching from eastern Texas to southern Virginia. Over the past two centuries, urban and agricultural development, timber harvest, and fire suppression have reduced the extent of these forests by almost 97 percent (Longleaf Alliance, 2015). The species extensive historical range demonstrates its ability to thrive on a variety of soils within the Southeast, ranging from the xeric sandy Entisol soils of the Coastal Plain to the mesic clayey Ultisol soils of the Piedmont and the wet mesic Spodosols of the Flatwoods region (Mclntyre et. al. 2008; Peet 2006).

The U.S. Southeast is not homogeneous but includes eight different physiographic regions and a wide variety of soil series. Longleaf pine (LLP) site zones identified by Craul et al. (2005), the vegetation classifications of Peet and Allard (1993), and the ecological classification system of Peet (2006) all recognize the intrinsic climatic and soil variability of the Southeast and incorporate it into these classification systems. In this study, we focus on LLP ecosystems within the Piedmont Plateau, and the Middle Coastal Plain regions. The Piedmont Plateau region is bordered to the west by the Appalachian Mountains and to the east by the Coastal Plain. This landscape is mostly formed on granite, but does have other crystalline bedrock, and has well-developed drainage networks with complex topography. The moderate-relief landscape found in the Piedmont is a result of millions of years of erosion, gradually transforming mountains into a rolling landscape. The Middle Coastal Plain is situated between the Piedmont and the flattest portions of the Lower Coastal Plain closest to the coast. Sediments here are

marine deposits of sand, silt, clay, and gravel. The region is generally of low-relief with steeper slopes near stream channels. The soils in the Piedmont differ from those in the Middle Coastal Plain due to the contrasting geologies of bedrock vs marine deposits. In the Piedmont soils are predominantly in the Ultisol and Alfisol orders whereas in the Middle Coastal Plain Ultisols and Entisol (Quartzpsamments) are common (Craul et al., 2005).

Regeneration and restoration of the LLP ecosystem in these regions has become an important goal among many groups and government agencies such as the Longleaf Alliance, National Fish and Wildlife Foundation, The Nature Conservancy, U.S. Forest Service, and the Natural Resource Conservation Service (NRCS). The NRCS, in particular, participated in the Conservation Reserve Program's Longleaf Pine Initiative (LLPI) that started in 2006 to plant marginal agricultural lands to LLP and in 2010 the NRCS extended the LLPI to foster regeneration and restoration of LLP on private lands. Regeneration of LLP is typically accomplished through planting of seedlings while restoration is most often through the re-introduction of prescribed fire, as longleaf pine ecosystems are considered fire maintained (Platt et. al., 1988). Prescribed fires reduce competing vegetation, prepare soils for seeds, provide space for a wide variety of endemic understory vegetation, and enhance the open savannah-like structure of many LLP forests (Kavanagh et al. 2010). Fire is not the only way to induce LLP restoration; for example, the NRCS also promotes forest stand improvement through thinning or hardwood removal, restoration and management of rare or declining habitats, and tree/shrub establishment (NRCS, 2011).

The historical range of the longleaf pine ecosystem has been designated a priority landscape by the NRCS and they have worked to develop a range of state-and-transition-models that identify expected transitions in ecological site conditions with a change in management (i.e., agricultural abandonment or introduction of fire). When considering restoration and regeneration of LLP within this framework of state-transitions for a particular ecological site there is an interest in understanding how soil characteristics may vary with landscape position, and thus impact LLP communities, and how changing management will change soil properties. The state-and-transition models are designed for specific physiographic settings and ecological site descriptions (ESD) that are predominantly defined by plant communities but also by soil properties (Caudle et al. 2013).

Across the Southeast region, soil moisture and percent silt were identified as critical attributes distinguishing the plant communities of LLP ecosystems, both plant community composition and productivity were distinguished by these attributes (Peet 2006). Working in the Middle Coastal Plain of Georgia, both soil moisture and topographic relief class (steeply sloping {> 8%}, undulating {> 3-8%}, or nearly level {1-3%}) were found to influence overstory species diversity (Kirkman et al. 2004). Other studies have looked at the role of landscape position on soil attributes in LLP landscapes. Greater soil C contents were found in bottomlands, compared to uplands, with similar management in the Middle Coastal Plain region of GA (Silveira et al 2009). Another study extended the upslope-downslope comparison into depressional wetlands and demonstrated increased soil C in wetlands as well as lower N mineralization and higher

extractable P (Craft and Chiang, 2002). These landscape and gradient studies make inferences about LLP ecosystems at the level of soil orders and soil series.

In contrast to the above broad soil comparisons, studies that have investigated changes in soil properties under LLP with changes in management, often limit investigation to a single or a few soil series. A study in South Georgia, for example, investigated changes in soil attributes under LLP after agricultural abandonment and reported working only on two closely related series of Wagram (Loamy, kaolinitic, thermic Arenic Kandiudult) and Norfolk (Fine-loamy, kaolinitic, thermic Typic Kandiudult) (Will et al. 2002). Similarly, another study working at the Savannah River Site in South Carolina investigating fire frequency and land use history impacts on soil under LLP focused on Blanton (Loamy, siliceous, semiactive, thermic Grossarenic Paleudults) and Fuquay (Loamy, kaolinitic, thermic Arenic Plinthic Kandiudults) series (Bizzari et al., 2015; Soil Survey Staff, 1999).

When studying dynamic soil properties (DSP; i.e., properties that are expected to change on human timescales of decades to centuries) such as pH or organic carbon it is recommended that studies focus on specific soil map units, specifically the series (Tugel et al., 2008). However, this recommendation does not address the fact a soil series is only one component of a map unit. Differences in slope, historic erosion or other features indicated by the map unit may be as, or more important, than the soil series itself for determining vegetation-soil relationships (Soil Survey Division Staff, 1993). As such, when studying DSPs under LLP one might keep the soil series consistent while sampling

across different map unit phases with varying slope, which as noted above can impact both LLP communities and soil attributes.

Presently, there is little research concerning how soil map units relating to slope steepness within a soil series might impact inferences about LLP community classification or about DSP under LLP regeneration or restoration. In this study we analyze how adjoining map units vary in slope steepness at four different sites, two located within the Piedmont/Upper Coastal Plain region and two within the Coastal Plain region of Georgia, differ in several dynamic soil properties. This study also incorporates the use of visible/near-infrared (VNIR) spectroscopy as a rapid, field based approach for analyzing soil properties of interest (i.e., carbon, clay, and pH_{cacl2}) that may help evaluate soil variability across slope steepness or dynamic soil properties over time. Based on previous research on landscape position we hypothesized that slope steepness across map units would differ in soil properties affecting soil moisture (i.e., clay) and that pH_{cacl2} and C would be higher in map units with the lowest slope.

Methods

Study Sites

This study was conducted using four locations within Georgia. Two sites were located within the Piedmont/Upper Coastal Plain, and two in the Middle Coastal Plain (Figure 3.1). The sites within the Piedmont/Upper Coastal Plain region were located in Hancock County and in Jones County at the Hitchiti Experimental Forest within the Oconee National Forest located near Juliette (Figure 3.2 and 3.3). The two sites located

in the Middle Coastal Plain region were located within the Ohoopee Dunes Natural Area near Swainsboro and the Joseph W. Jones Ecological Research Center at Ichauway in Newton (Figure 3.4 and 3.5). All sites were dominated by an overstory of longleaf pine, although the Piedmont/Upper Coastal Plain sites were planted 8 and 16 years ago while the Coastal Plain stands were a more mature, naturally regenerated stand with many trees >40 years old. The Hitchiti and Hancock County sites are both cutover sites converted from loblolly pine stands (*Pinus taeda* L.) to longleaf pine. The Ohoopee Dunes site is managed by the Georgia Department of Natural Resources as a conservation area with some use of prescribe fire while the Jones Center has minimal harvest and is managed with prescribed fire on a two or three year return interval. The Jones Center site had been recently burned prior to sampling.

The soil within the Hitchiti site consist of the Vance soil series, which is a fine, mixed, semiactive, thermic Typic Hapludult commonly found within the Piedmont. The soil map units within this study site are VaB2 and VaC2, this notation indicates that the unit consists of the Vance series with a slope of 2-6% or 6-10%, respectively, and these units are eroded. The Hancock County site contains the Bonifay soil series, common to the Upper Coastal Plain, which is a loamy, siliceous, subactive, thermic Grossarenic Plinthic Paleudult. The Grossarenic designation indicates that the profile has a sandy layer between 100 and 150 cm thick. The soil map units of interest within this site are BnB and BnD, indicating slopes of 0-6 or 6-12%, respectively. The Ohoopee Dunes site also consists of the Bonifay soil series, but with different map unit notation, which can be common between counties. The map units of interest within this site are BoB, BoC, and

BoD, which indicates that the units are slopes of 0-5, 5-8, and 8-12%, respectively. Lastly, the Jones Center site is comprised of the Troup soil series, which is a loamy, kaolinitic, thermic Grossarenic Kandiudult, a series commonly found within the Coastal Plain. The map units of interest are TwB and TwC indicating slopes of 0-5 and 5-8%, respectively. These soil series descriptions are based on USDA-NRCS Soil Survey Division (https://soilseries.sc.egov.usda.gov).

Soil Sampling

In each map unit two or three sampling locations were randomly selected. These random selections in the map units were not always consistent with the slope designation but the locations were maintained and these few discrepancies are described below. Given our interest in the designation of soil maps units and DSPs we sampled complete soil profiles in each location. Mineral soils were sampled at 12 different depths: 0-2, 9-11, 0-20, 20-40, 40-60, 60-80, 80-100, 100-120, 120-140, 140-160, 160-180, and 180-200 cm. For the upper two depths, a soil punch tube with 2 cm diameter was used and 3-5 cores per sampling location were composited. For the 20-cm increment samples, a 6-cm diameter soil auger was utilized. Sampling location VaC2-3 was an exception to this method and was only sampled to 120 cm in depth due to the inability to auger through weathered bedrock.

A VNIR field Spectrophotometer (Analytical Spectral Devices, Boulder, Co.) with Indico Pro software was used to scan soil samples in the field. The VNIR Spectrophotometer scans soils from 350 to 2500 nm in 1 nm increments using a contact

probe. The probe has a window diameter of 2 cm. The scans were completed by first performing a baseline scan using a Spectralite white blank (ASD, Inc.). The lens of the contact probe was pressed firmly against the surface of the soil sample within its sample bag, so that no light from the lens was visible. Soil within the sample bag was mixed, and the refreshed surface was scanned again. Each spectrum was averaged from a compilation of 50 readings during each scan. This was performed three times per sample and the three scans were then averaged. Between each sample, the contact probe was cleaned. A baseline scan was performed after every 10 samples.

Stand Attributes

In each plot, all individual trees within a radius of 10m from the plot center and a diameter at breast height (DBH) greater than 4 cm were identified and measured for DBH to determine basal area. Stem density was calculated within a diameter of 10 m by counting all stems with a height>1m and dividing by the area (m^2). Ground cover was determined for a 10 m transect in both the eastward and westward direction from plot center, totaling 20 m of transect. Ground cover directly below each meter along the transects was classified as green/living, bare soil, or forest floor. A percentage was calculated for each category. Lastly, two or three dominant tree heights and two or three codominant tree heights were measured within the 20 m diameter plot.

Soil Analysis

Samples were air-dried before being ground and passed through a 2-mm sieve. Jones Center sampling depths of 20-40, 60-80, 100-120, 140-160, and 180-200 cm for all locations were not included within this analysis. A moisture correction factor was determined for each air-dried soil sample by placing 3-6 g in tin cups and drying until a constant weight at 105^0C. Soils were analyzed for pH, C and nitrogen (N), particle size distribution, and exchangeable acidity. Soil pH_{H2O} and pH_{CaCl2} were measured using a 1:1 ratio of soil and deionized (DI) water or 0.01 M $CaCl_2$ following Thomas (1996). C and N concentrations were obtained from a Flash 2000 Series CN soil analyzer (CE Elantech, Lakewood, NJ). Particle size distribution was measured using the hydrometer method (Gee and Or, 2002). Exchangeable acidity values were obtained by shaking 5 g of soil with 50 mL of 1 M KCl and filtering through a Whatman 42 filter. Extracts were titrated to a pH of 8.2 with 0.02 M NaOH using an auto-titrator (Metrohm-Toledo, Columbus, OH) (Bertsch and Bloom, 1996).

Statistical and Data Analysis

Soil Map Units were sorted into 3 slope categories: Flat, Medium, and Steep, containing slopes ranging approximately from 0-6, 6-8, and 8-12%, respectively. Results were analyzed by depth as a randomized block design, with soil chemical and physical comparisons made between Region and Map Unit Slope with site as the blocking factor. Data were compared using a full interaction analysis of variance (ANOVA) across both regions and all slope categories. Pairwise comparisons were tested for significant

difference at $p<0.05$ using Tukey's Honestly Significant Difference (HSD). Stand attributes were also analyzed using this method to determine significance between basal area and ground coverage with region and slope as described above. VNIR calibration and analysis processes can be found in more detail in chapter two of this thesis. Raw reflectance spectra were preprocessed by cleaning and smoothing in R version 3.2.3, and using Savitzky-Golay (SG), continuum removal (CR), or wavelets (WT) transformations. Spectra and percent clay, % C, or pH_{cacl2} data were randomly separated into 20% test and 80% training datasets. To avoid splitting up soil profiles within these sets, the Kennard-Stone Algorithm was used (Kennard & Stone, 1969). PLSR (Partial Least Square Regression) or SVM (Support Vector Machine) was used to perform the calibration. Coefficients of determination (R^2) and the root mean square error (RMSE) were used to compare the results. The best calibration was determined for All data, Piedmont/Upper Coastal Plain samples, and Coastal Plain samples. Data were analyzed using R version 3.2.3, and ArcMap version 10.3.

Results

Soil Profile Attributes

Measured soil attributes across the sites and over depth ranged broadly (Table 3.1 and Table 3.2). Percent clay, for example, ranged from <1% to over 70%. Between the regions clay content was statistically greater in the Piedmont/Upper Coastal Plain versus the Coastal Plain by ~15% within the 40-60 cm depth range and by ~13% within the 80-100 cm depth (p= 0.008 and 0.03, respectively). Other depths were not statistically

different between the regions. For slope steepness, percent clay was ~20% lower ($p=0.045$) when comparing Steep slope to Flat slope, in the 180-200 cm depth range (Figure 3.6). Again, other depths were not statistically different for percent clay among steepness. Within specific sites, map unit profiles did not vary consistently for clay. At the Hitchiti site, between map units, VaB2 (rep 1 and 2) had clay concentrations between 40 and 60 %, while VaC2 (rep 1 and 2) had 30 to 40% clay, which is consistent with a Bt horizon for a Vance soil series. However, VaC2-3 only contained 10% clay at this Bt horizon depth (Figure 3.7). For the Hancock County site, percent clay was generally low (1-5%) in the upper 40 cm but increased to a peak of 70% clay within the 120-160 cm depth (Figure 3.7). Variance with slope steepness was inconsistent at this site. Within the Ohoopee Dunes, percent clay generally increased with depth for all map units, with the exception of BoD-1 and BoD-2, which had very little clay present (Figure 3.7). Within the Jones Center site, percent clay increased relatively consistently with depth and ranged from 0- 30% (Figure 3.7).

Percent soil C was significantly different between the regions in 0-2, 9-11, and 40-60 cm depths ($p= 0.02$,0.04, and 0.02, respectively). Differences by slope steepness were only significant in 9-11 cm ($p=0.0004$) but was not different at deeper depths. Percent soil C within the 9-11 cm range was 47% lower in the Piedmont/Upper Coastal Plain than the Middle Coastal Plain. For the slope comparison, Medium slope was 62% higher than the Flat slope and 78% higher than the Steep slope ($p = 0.017$ and 0.0017, respectively). In all the sites % C declined steadily with depth for each profile (Figure

3.8) except for the Ohoopee Dunes where percent C decreased with depth until the 180 cm depth but increased slightly within the 180-200 cm depth (Figure 3.8).

Finally, pH_{cacl2} exhibited no significant differences for any depth across region or slope. At the Hitchiti site there was a distinct increase when comparing VaC2 to VaB2, with VaC2 pH increasing with depth (Figure 3.9) but for all other sites pH remained fairly consistent with depth for all map units.

Stand Attributes

Stand data attributes varied widely, particular for basal area, which ranged from <0.02 to 30 m^2 ha^{-1}. Despite this variance across the sites neither region nor slope steepness were significantly different for basal area. There were also no statistically significant differences for tree height, stem density, or ground cover for region or slope (Table 3.2).

VNIR Analysis

Field based VNIR calibrations and validations focused on percent clay for soil map unit classification purposes while calibration for DSP used soil C and pH. The analysis investigated calibrations over all the data as well as by region (Piedmont/Upper Coastal Plain or Coastal Plain). For all percent clay data, partial least squared regression (PLSR) with Continuum Removal (CR) yielded R^2 = 0.68 on validation data compared to 0.70 and 0.64, respectively, for Sovitzky Golay (SG) and Wavelet transformation (WT) transformations. In contrast, support vector machine (SVM) with CR yielded R^2 = 0.40,

compared to 0.70 and 0.72 for SG and WT. For Piedmont/Upper Coastal Plain percent clay, PLSR with CR yielded R^2 = 0.96 on validation data compared to 0.85 and 0.93 for SG and WT. SVM produced fits yielding R^2 = 0.88, 0.52, and 0.67 for CR, SG, and WT. For Coastal Plain percent clay, PLSR with CR yielded R^2 = 0.91 on validation data compared to 0.76 and 0.70 for SG and WT, and SVM yielded R^2 = 0.42, 0.55 and 0.43 for CR, SG and WT, respectively (Table 3.3; Figure 3.10). All percent clay data analyses also resulted in higher *RMSE* fits than either Piedmont/Upper Coastal Plain or the Coastal Plain analyses alone (Table 3.3).

For all percent C data, PLSR with CR yielded R^2 = 0.48 on validation data compared to 0.16 and 0.55 for SG and WT transformations. In contrast, SVM with CR yielded R^2 = 0.11, compared to 0.27 and 0.54 for SG and WT. For Piedmont/Upper Coastal Plain percent C, PLSR with CR yielded R^2 = 0.33 on validation data compared to 0.43 and 0.67 for SG and WT. SVM produced much poorer fits, yielding R^2 = -0.19, 0.25, and 0.43 for CR, SG, and WT, respectively. For Coastal Plain percent C, PLSR with CR yielded R^2 = 0.51 on validation data compared to 0.18 and 0.73 for SG and WT, and SVM yielded R^2 = 0.26, 0.37 and 0.58 for CR, SG and WT (Table 3.4; Figure 3.11). *RMSE* fits were smaller for validation results with R^2 decreasing from All to Piedmont/Upper Coastal Plain to Coastal Plain (Table 3.4).

Finally, for all pH_{CaCl2} data, PLSR with CR yielded R^2 = 0.14 on validation data compared to 0.19 and 0.20 for SG and WT transformations. In contrast, SVM with CR yielded R^2 = 0.12, compared to -0.25 and -0.05 for SG and WT. For Piedmont/Upper Coastal Plain pH_{CaCl2}, PLSR with CR yielded R^2 = 0.15 on validation data compared to

0.62 and 0.05 for SG and WT. SVM produced much poorer fits, yielding R^2 = -0.33, 0.09, and -0.11 for CR, SG, and WT. For Coastal Plain pH_{CaCl2}, PLSR with CR yielded R^2 = 0.54 on validation data compared to 0.14 and 0.08 for SG and WT, and SVM yielded R^2 = 0.20, 0.01 and 0.09 for CR, SG and WT (Table 3.5; Figure 3.12). All pH_{CaCl2} data analyses generally resulted in higher *RMSE* fits than either Piedmont/Upper Coastal Plain or the Coastal Plain analyses (Table 3.5).

Discussion

In this study, we focused on soil variance across soil map unit phases of slope steepness within a soil series as it might relate to understanding changes in dynamic soil properties during LLP regeneration or restoration. We characterized 2 m profiles in adjoining map units to understand how well soil maps units, as delineated by polygons on soil maps, accurately capture variance over slope steepness and how surface soil variance across these units might impact our ability to quantify soil change. We also measured all soil with VNIR to assess how well this rapid field technique could measure soil attributes of interest (i.e., clay, C, and pH) both for field classification of soils and measurement of DSP over time.

When considering sharply delineated polygons of soil map units, it is well recognized that such classifications are not 100% pure and will contain inclusions of other soil series or other soil phases (i.e., slopes) (Odgers et al., 2014; Burrough et al., 1997). Similarly, soil does not usually change abruptly at the polygon boundaries, although for slope boundaries might be more well defined (Greve and Greve, 2004). In

our study both issues of inclusions and boundary delineations were evident. At the Hitchiti site, for example, the profiles collected furthest down the hillslope (VaC2-3 and VaC2-2) have an increase in pH at depth unlike the other profile in the same map unit (VaC2-1), or the other two profiles in the adjacent map unit phase of the same soil series (VaB2-1 and VaB2-2). This, in part, may be due to surrounding mafic soils as represented by the Davidson (Fine, kaolinitic, thermic Rhodic Kandiudults) soil series (DhE2 in Figure 3.3). The Rhodic designation indicates a darker color in the Davidson from the mafic rock but may also cause the soil to become more basic with depth compared to the more acidic felsic soils located at the top of the hill slope that have a slightly declining pH with depth (Raulund-Rasmussen et al. 1998; Figure 3.9). Increasing pH with depth is characteristic of Alfisols. These types of inclusions might well impact community composition, as observed by Kirkman et al. (2004) at a slightly larger scale, but cannot be identified in the absence of even finer scale map units (Ogder et al., 2014).

Another map unit inconsistency was identified within the Ohoopee Dunes. Despite locating profiles BoD-1 and BoD-2 within the map unit boundary (Figure 3.3) the percent clay is well below the other four profiles in the adjacent Bonifay map units (Figure 3.7). In fact, these low clay profiles are not Bonifay as they do not possess an argillic horizon that would be defined by a 4% absolute increase in clay with depth (Soil Survey Staff, 1999). Thus, regardless of being located near the middle of the BoD map unit, these profiles display characteristics of the Kershaw soil series, which is present next to the BoD map unit. This BoD map unit was identified as being of 8-12% slope but

field observations clearly indicated inclusions of some slopes <8%. When using map units for investigations of slope steepness or DSP it is evident that units must be ground-truthed such that geographical delineations of mapping units are consistent with physiographic realities in the field. This caution is stated in the NRCS Soil Change Guide (Tugel et al., 2008) but is often ignored in modeling efforts that may, for example, be interested in estimating soil C sequestration with LLP regeneration across the region.

The two examples above demonstrate some of the potential utility in developing VNIR for field use. In the first example an ability to measure pH in the field might help identify changes in underlying bedrock, which may alter LLP regeneration or restoration objectives. The VNIR calibrations for pH across all data were poor (R^2=0.2) but separating the data into Piedmont/Upper Coastal Plain and Coastal Plain regions yielded improved results (R^2=0.62 and 0.54, respectively) (Figure 3.12). Although these validation results are below what is desired for a predictive model (i.e., R^2 >0.8), they are promising and still might detect a pH change from 4 to 6 as observed in the Hitchiti. The ability to measure pH as a DSP under LLP regeneration or restoration would also be beneficial. Declines in surface soil (0-10 or 0-15 cm) pH have been observed under LLP regeneration on post-agricultural land compared to reference LLP (Bizzari et al., 2015; Will et al., 2002), although in both these cases pH decreases ranged from 4.8 to 4.0 or 4.7 to 4.5. To identify such changes in pH, VNIR prediction models will need to improve.

In the second example above, the ability to measure soil percent clay in the field might prove useful. Of the three soil characteristics measured, VNIR predicted percent clay best with validations of R^2 =0.72, 0.96, and 0.91 for All Data, Piedmont/Upper

Coastal Plain, and Coastal Plain datasets, respectively. Previous VNIR models for clay measurement have also been successful (Waiser et al., 2007). The VNIR could be used to more easily classify soils within the field. For example, VNIR may enable a user to determine if and where the argillic horizon starts within a profile, which might help distinguish between an Arenic or Grossarenic designation. Similarly, distinguishing between sandy series such as Kershaw (Thermic, uncoated Typic Quartzipsamments) or Lakeland (Thermic, coated Typic Quartzipsamments) that are separated by having less than or greater than 5% silt + clay might be possible in the field. This information could aid with soil mapping and thus regeneration or restoration management decisions (Waiser et al. 2007).

The final VNIR calibration was for soil total C, a DSP of particular interest. Prediction models with the PLSR and WT transformation performed best with R^2 for validations of 0.55, 0.67, and 0.73 for All, Piedmont/ Upper Coastal Plain, and Coastal Plain, respectively (Figure 3.11). The Coastal Plain calibration contained the highest and best validation and cross-validation R^2. Being able to accurately estimate soil C within the field quickly and cheaply will help determine how LLP regeneration or restoration may be altering C concentrations or contents, which plays a fundamental role in soil fertility. Also, knowing the amount of C being stored during LLP regeneration or restoration has taken on a particular interest relative to atmospheric CO_2 concentration and fire management (Longleaf Alliance, 2015; Lavoie et al. 2014; Mississippi Forestry Commission, 2008).

Previous studies within LLP have clearly demonstrated changes in soil C with regeneration, fire, and landscape position. For example, in the Middle Coastal Plain of SC soil on post-agricultural lands regenerating with LLP had 0-15 cm soil C values of 0.9 % compared to reference LLP of 1.35% (Bizzari et al., 2015). In the Middle Coastal Plain of GA similar results were observed for 0-10 cm soil in regenerating stands (0.6 ± 0.6% C) relative to reference stands (2.19±0.19% C) (Will et al., 2002). In this same GA location LLP in the absence of fire had 2.57% C while regularly burned reference stands had 1.7% C (Boring et al., 2016). Finally, relative to 0-20 cm upland soils (1.29 ± 0.6 % C) bottomland soils were three-fold higher (4.79±5.61 %C) (Silviera et al. 2009). The VNIR calibrations should be able to detect these size difference (Figure 3.11), although quantitative prediction will require some refinement of these C models.

Relative to our primary interest of map units and slope steepness, surface soil C (0-2, 9-11, or 0-20 cm) did not vary consistently with slope (Figure 3.6). In the 0-2 cm layer soil C increased with slope steepness but not significantly (Figure 3.6). Only in the 9-11 cm layer was slope significant and here the middle steepness showed the highest soil C, which is not consistent with our original hypothesis. Whether variance in these map units with slope steepness can inform changes in DSP during LLP regeneration or reforestation depends on the variance in the units (or strata) compared to the overall landscape variance. When measuring 186 samples in an upland to bottomland gradient study, the coefficient of variation (CV) for soil C was 144% over all samples and 50 or 118% in the upland and bottomland, respectively (Silviera et al. 2009). This is similar to the results of our study. The percent C CV over all soil profiles for 0-2, 9-11, or 0-20 cm

depths was 127%, 92%, and 58%, respectively (n = 22 per depth increment). Within the slope classes of flat, medium, or steep the CV for soil C is 49%, 28%, or 150%, 29%, 68%, or 46%, and 58%, 70%, or 47% for 0-2 (n= 10 per slope class), 9-11 (n= 5 per slope class), and 0-20 cm (n = 7 per slope class), respectively. The 9-ll cm depth contains smaller CV across slope class than the CV for all samples combined for 9-11 cm. This further supports the significance of slope class within the 9-ll cm depth. In relation to DSPs, it would appear that the smallest scale of soil classification, soil map unit phases, may not be beneficial for improving our ability to determine soil property change over time under longleaf regeneration or restoration. There is too much variance within the soil map unit phases for the inclusion of slope to improve statistical models.

Conclusion

This study suggests that soil map unit phases capturing steepness of slope will not be a valuable stratification variable in analyzing DSP under LLP regeneration or restoration. Few significant differences were observed between slope classes at any depth (0-200 cm) for the measured variables (percent clay, C, pH) and even in cases of observed differences there was not a clear monotonic pattern from flat to steep. VNIR calibrations for percent clay demonstrated potential predictive value (i.e., $R^2 \geq 0.9$) while those for C and pH, although not as strong, indicated some utility for field classification or monitoring of DSP.

References

Bertsch, P.M., Bloom, P.R., (1996). Aluminum. In: Sparks, D.L., Page, A.L., Helmke, P.A., Loeppert, R.H. (Eds.), Methods of Soil Analysis Part 3—Chemical Methods. Soil Science Society of America, American Society of Agronomy, Madison, WI.

Bizzari, L. E., Collins, C. D., Brudvig, L. A., & Damschen, E. I. (2015). Historical agriculture and contemporary fire frequency alter soil properties in longleaf pine woodlands. *Forest Ecology and Management*, 349: 45-54.

Boring, L., Starr, G., Staudhammer, C. L., Wiesner, S., Kunwor, S., Loescher, H. W., & Baron, A. F. (2016). Carbon Dynamics of *Pinus palustris* Ecosystems Following Drought. *Forests*, *7*(5): 98.

Burrough, P. A., van Gaans, P. F., & Hootsmans, R. (1997). Continuous classification in soil survey: spatial correlation, confusion and boundaries. *Geoderma*, 77(2): 115-135.

Caudle, D., Sanchez, H., DiBenedetto, J., Talbot, C., & Karl, M. S. (2013). *Interagency ecological site handbook for rangelands*. US Department of the Interior, Bureau of Land Management.

Craft, C. B., & Chiang, C. (2002). Forms and amounts of soil nitrogen and phosphorus across a longleaf pine–depressional wetland landscape. *Soil Science Society of America Journal*, *66*(5): 1713-1721.

Craul, P. J., Kush, J. S., & Boyer, W. D. (2005). *Longleaf pine site zones* (Vol. 89). USDA Forest Service, Southern Research Station.

Fox, C. A., Tarnocai, C., Broll, G., Joschko, M., Kroetsch, D., & Kenney, E. (2014). Enhanced A Horizon Framework and Field Form for detailed field scale monitoring of dynamic soil properties. *Canadian Journal of Soil Science*, 94(2): 189-208.

Gee, G. W., and Or, D. (2002). 2.4 Particle-Size Analysis. Methods of Soil Analysis: Part 4 Physical Methods sssabookseries:255-293.

Greve, M. H., & Greve, M. B. (2004). Determining and representing width of soil boundaries using electrical conductivity and MultiGrid. *Computers & Geosciences*, 30(6): 569-578.

Jiménez, J. J., Lal, R., Leblanc, H. A., & Russo, R. O. (2007). Soil organic carbon pool under native tree plantations in the Caribbean lowlands of Costa Rica. *Forest Ecology and Management*, 241(1): 134-144.

Karlen, D. L., Ditzler, C. A., & Andrews, S. S. (2003). Soil quality: why and how? Geoderma, 114(3): 145-156.

Kavanagh, K., Koyama, A., & Stephan, K. (2010). After the Fire, Follow the Nitrogen. Retrieved December 1, 2015, from https://www.firescience.gov/projects/briefs/04-2-1-97_FSBrief92.pdf

Lavoie, M., Mack, M. C., Hiers, J. K., Pokswinski, S., Barnett, A., & Provencher, L. (2014). Effects of restoration techniques on soil carbon and nitrogen dynamics in Florida longleaf pine (*Pinus palustris*) sandhill forests. *Forests*, 5(3): 498-517. doi:10.3390/f5030498

Longleaf Alliance. (2015). *About Longleaf*. Retrieved from http://www.longleafalliance.org/

Mclyntyre, R.K; Jack, S.B; Mitchell, R.J.; Hiers, J. K.; Neel, W.L. (2008). Multiple Value Management: The Stoddard~ Neel Approach to Ecological Forestry in Longleaf Pine Plantations. *Joseph W. Jones Ecological Research Center*. Retrieved from http://www.americaslongleaf.org/media/3536/multiple_value_management_the_stoddard-neel_approach_to_ecological_forestry.pdf

Mississippi Forestry Commission (2008). Benefits of Prescribed Fire Longleaf Pine. Retrieved December 3, 2015, from http://www.mfc.ms.gov/pdf/Pubs/Benefits_Prescribed_Burning_LL_Pines.pdf

Mora, J. L., Guerra, J. A., Armas-Herrera, C. M., Arbelo, C. D., & Rodriguez-Rodriguez, A. (2014). Storage and depth distribution of organic carbon in volcanic soils as affected by environmental and pedological factors. *Catena [Giessen*], 123: 163-175. doi:10.1016/j.catena.2014.08.004

Natural Resource Conservation Service (NRCS). (2008). *Soil Quality Physical Indicators: Selecting Dynamic Soil Properties to Assess Soil Function.* Retrieved from http://www.nrcs.usda.gov/Internet/FSE_DOCUMENTS/nrcs142p2_050948.pdf.

Natural Resource Conservation Service (NRCS). (2011). *Longleaf Pine Initiative.* Retrieved from http://www.nrcs.usda.gov/wps/portal/nrcs/detailfull/national/home/?cid=nrcsdev11_023913.

Odgers, N. P., Sun, W., McBratney, A. B., Minasny, B., & Clifford, D. (2014). Disaggregating and harmonising soil map units through resampled classification trees. Geoderma, 214: 91-100.

Peet, R. K., & Allard, D. J. (1993, May). Longleaf pine vegetation of the southern Atlantic and eastern Gulf Coast regions: a preliminary classification. In Proceedings of the Tall Timbers fire ecology conference (Vol. 18, pp. 45-81).

Peet, R. K. (2006). Ecological classification of longleaf pine woodlands. In *The Longleaf Pine Ecosystem* (pp. 51-93). Springer New York.

Platt, W.J., Evans, G.W., and Rathun, S.L. (1988). The population dynamics of a long lived conifer (*Pinus palustris*). *American Naturalist* 131(4): 491-525.

Quijano, L., Gaspar, L., & Navas, A. (2016). Lateral and depth patterns of soil organic carbon fractions in a mountain Mediterranean agrosystem. *Journal of Agricultural Science*, 154(2): 287-304.

Raulund-Rasmussen, K., Borggaard, O. K., Hansen, H. B., & Olsson, M. (1998). Effect of natural organic soil solutes on weathering rates of soil minerals. *European Journal of Soil Science*, 49(3): 397-406.

Ritchie, J. C., McCarty, G. W., Venteris, E. R., & Kaspar, T. C. (2007). Soil and soil organic carbon redistribution on the landscape. *Geomorphology*,89(1): 163-171.

Silveira, M. L., Comerford, N. B., Reddy, K. R., Prenger, J., & DeBusk, W. F. (2009). Soil properties as indicators of disturbance in forest ecosystems of Georgia, USA. *Ecological indicators*, *9*(4): 740-747.

Soil Survey Division Staff. (1993). Soil survey manual. Soil Conservation Service. U.S. Department of Agriculture Handbook 18.

Soil Survey Staff. (1999). Soil taxonomy: A basic system of soil classification for making and interpreting soil surveys. 2nd edition. Natural Resources Conservation Service. U.S. Department of Agriculture Handbook 436.

Thomas, G.W., (1996). Soil pH and Soil Acidity. In: Sparks, D.L., Page, A.L., Helmke, P.A., Loeppert, R.H. (Eds.), Methods of Soil Analysis Part 3—Chemical Methods (pp. 475-490). Soil Science Society of America, American Society of Agronomy, Madison, WI.

Tugel, A. J., Wills, S. A., and Herrick, J. E. (2008). Soil Change Guide: Procedures for Soil Survey and Resource Inventory, Version 1.1. USDA, Natural Resources Conservation Service, National Soil Survey Center, Lincoln, NE.

Waiser, T. H., Morgan, C. L. S., Brown, D. J., & Hallmark, C. T. (2007). In situ characterization of soil clay content with visible near-infrared diffuse reflectance spectroscopy. *Soil Science Society of America Journal*, 71(2): 389-396.

Will, R. E., Wheeler, M. J., Markewitz, D., Jacobson, M. A., & Shirley, A. M. (2002). II. Early loblolly pine stand response to tillage on the piedmont and upper coastal plain of Georgia: Tree allometry, foliar nitrogen concentration, soil bulk density soil mositure, and soil nitrogen status. *Southern Journal of Applied Forestry*,26(4): 190.

Table 3.1: Minimum and maximum values for soil characteristics across two Piedmont/Upper Coastal Plain and two Coastal Plain sites in GA collected in 2015/2016. (n= 278 for Carbon, Nitrogen, and Ex.Ac.; n= 226 for Clay and pH)

Depth	Clay (%)		[1]pH_{CaCl2}		Carbon (%)		Nitrogen (%)		[2]Ex.Ac. (cmol+/kg soil)	
(cm)	Min.	Max.	Min.	Max.	Min.	Max.	Min.	Max.	Min.	Max.
0-2	NA	NA	NA	NA	0.04	11.85	0.01	0.19	0.02	1.32
9-11	NA	NA	NA	NA	0.03	3.78	0.01	0.08	0.24	5.00
0-20	0.77	29.54	3.42	5.07	0.02	1.66	0.01	0.06	0.12	3.17
20-40	1.00	55.94	3.72	4.70	0.13	0.56	0.01	0.03	0.01	4.90
40-60	0.77	57.26	3.52	5.14	0.06	1.58	0	0.06	0.10	8.70
60-80	0.39	50.58	3.71	4.85	0.04	1.15	0	0.09	0.12	6.75
80-100	1.00	47.15	3.75	5.47	0.03	0.41	0	0.02	0.01	6.75
100-120	1.00	55.86	3.71	6.17	0.01	0.26	0	0.03	0.04	18.00
120-140	0.39	65.35	3.42	4.80	0	0.37	0	0.03	0.08	30.38
140-160	1.00	73.44	3.57	5.47	0	0.23	0	0.03	0.04	39.81
160-180	1.00	70.71	3.63	5.84	0	0.27	0	0.03	0.04	39.51
180-200	0.44	70.69	3.43	6.14	0.02	2.64	0	0.09	0.07	41.69

[1] pH measured in a 0.01 M $CaCl_2$ slurry
[2]Exchangeable acidity

Table 3.2: Stand characteristics and map unit slope for two Piedmont/Upper Coastal Plain (Hitchiti, Hancock) and two Coastal Plain (Ohoopee Dunes, Jones Center) sites in GA, taken at each soil profile sampling location in 2015/2016.

								Ground Cover		
Location	Map Unit	Rep.	Map Unit Slope	Soil Series	Basal Area	Tree Height	Stem Density	[1]FF	[2]GR	[3]BS
					m^2/ha	m	Stem/ha		%	
Ohoopee Dunes	BoD	1	Steep	Bonifay	2.88	21.20	509	90	0	10
	BoD	2	Steep	Bonifay	20.18	13.13	764	90	10	0
	BoC	1	Medium	Bonifay	16.47	18.97	891	65	35	0
	BoC	2	Medium	Bonifay	8.58	19.34	637	90	10	0
	BoB	1	Flat	Bonifay	18.33	15.03	1401	85	15	0
	BoB	2	Flat	Bonifay	1.45	11.93	637	90	10	0
Jones Center	TwC	1	Medium	Troup	1.504	11.04	2165	0	10	90
	TwC	2	Medium	Troup	0.074	2.80	762	0	25	75
	TwC	3	Medium	Troup	0.080	3.40	382	30	10	60
	TwB	1	Flat	Troup	0.232	4.43	3183	40	10	50
	TwB	2	Flat	Troup	0.000	23.16	509	40	10	50
	TwB	3	Flat	Troup	0.023	2.11	1655	35	5	60
Hitchiti	VaC2	1	Steep	Vance	0.039	12.28	4329	20	80	0
	VaC2	2	Steep	Vance	0.030	3.60	5474	40	60	0
	VaC2	3	Steep	Vance	0.039	3.08	3310	10	85	5
	VaB2	1	Flat	Vance	0.021	3.67	6366	40	60	0
	VaB2	2	Flat	Vance	0.078	4.60	2674	55	45	0
Hancock County	BnB	1	Flat	Bonifay	7.83	10.46	NA	25	70	5
	BnB	2	Flat	Bonifay	28.70	5.91	NA	40	30	30
	BnB	3	Flat	Bonifay	26.40	4.57	NA	20	55	25
	BnD	1	Steep	Bonifay	15.95	25.30	NA	25	70	5
	BnD	2	Steep	Bonifay	17.22	3.60	NA	60	30	10

1 Forest Floor
2 Green vegetation
3 Bare Soil

Table 3.3: Prediction results of validation and cross-validation RMSE and R^2 for each data separation, method, and transformation combination for percent clay, separated by all data, Piedmont/Upper Coastal Plain sites, and Coastal Plain sites. Methods: Partial Least Square Regression (PLSR) and Support Vector Machine (SVM). Transformations: Continuum Removal (CR), Savitzky-Golay (SG), and Wavelets (WT) (n_{All} = 226, $n_{Piedmont/Upper\ Coastal\ Plain}$ = 116, $n_{CoastalPlain}$= 105). N-comp is principle components utilized. Bold numbers highlight the best model result.

				Validation		Cross-Validation	
Data	**Method**	**Transformation**	**N Comp**	**R^2**	**RMSE**	**R^2**	**RMSE**
All	PLSR	CR	12	0.68	0.4188	0.91	0.5395
		SG	3	0.70	0.8581	0.95	1.0391
		WT	4	0.64	1.1311	0.92	1.0299
	SVM	CR		0.40	0.3929	0.88	0.5064
		SG		0.70	0.8483	0.93	0.9981
		WT		**0.72**	**0.9719**	**0.93**	**1.0281**
Piedmont/ Upper Coastal Plain	PLSR	CR	**8**	**0.96**	**0.5398**	**0.96**	**0.5631**
		SG	6	0.85	1.2284	0.99	1.2218
		WT	13	0.93	1.1027	0.96	1.2336
	SVM	CR		0.88	0.5479	0.90	0.5296
		SG		0.52	1.1999	0.96	1.2169
		WT		0.67	1.1735	0.95	1.2259
Coastal Plain	PLSR	CR	**8**	**0.91**	**0.4586**	**0.94**	**0.4615**
		SG	6	0.76	0.7027	0.98	0.8357
		WT	13	0.70	0.6827	0.96	0.8392
	SVM	CR		0.42	0.4912	0.79	0.5205
		SG		0.55	0.5694	0.89	0.7687
		WT		0.43	0.5409	0.89	0.7716

Table 3.4: Prediction results of validation and cross-validation RMSE and R^2 for each data separation, method, and transformation combination for percent C, separated by all data, Piedmont/Upper Coastal Plain sites, and Coastal Plain sites. Methods: Partial Least Square Regression (PLSR) and Support Vector Machine (SVM). Transformations: Continuum Removal (CR), Savitzky-Golay (SG), and Wavelets (WT) (n_{All} = 277 $n_{piedmont/Upper\ Coastal\ Plain}$= 139, $n_{coastalPlain}$= 137). N-comp is principle components utilized. Bold numbers highlight the best model result.

				Validation		Cross-Validation	
Data	**Method**	**Transformation**	**N Comp**	**R^2**	**RMSE**	**R^2**	**RMSE**
All	PLSR	CR	15	0.48	1.8963	0.71	1.7351
		SG	4	0.16	0.9526	0.88	0.9936
		WT	**5**	**0.55**	**0.8840**	**0.80**	**0.9492**
	SVM	CR		0.11	1.6591	0.55	1.7019
		SG		0.27	0.7858	0.79	0.9453
		WT		0.54	0.8881	0.77	0.9088
Piedmont / Upper Coastal Plain	PLSR	CR	9	0.33	1.8042	0.92	1.7497
		SG	10	0.43	1.0136	0.96	0.8861
		WT	**11**	**0.67**	**0.8906**	**0.93**	**0.8985**
	SVM	CR		-0.19	1.6391	0.76	1.7246
		SG		0.25	0.7655	0.88	0.8647
		WT		0.43	0.7265	0.88	0.8777
Coastal Plain	PLSR	CR	10	0.51	1.9750	0.82	1.7625
		SG	6	0.18	0.8305	0.96	1.1015
		WT	**3**	**0.73**	**0.9996**	**0.86**	**1.0217**
	SVM	CR		0.26	1.8492	0.59	1.7072
		SG		0.37	0.7672	0.78	0.9967
		WT		0.58	0.9021	0.74	0.9411

Table 3.5: Prediction results of validation and cross-validation RMSE and R^2 for each data separation, method, and transformation combination for pH_{CaCl2}, separated by all data, Piedmont/Upper Coastal Plain sites, and Coastal Plain sites. Methods: Partial Least Square Regression (PLSR) and Support Vector Machine (SVM). Transformations: Continuum Removal (CR), Savitzky-Golay (SG), and Wavelets (WT) (n_{All} = 226 $n_{piedmont/Upper\ Coastal\ Plain}$ = 116, $n_{coastalPlain}$= 105). N-comp is principle components utilized. Bold numbers highlight the best model result.

				Validation		Cross-Validation	
Data	**Method**	**Transformation**	**N Comp**	**R^2**	**RMSE**	**R^2**	**RMSE**
All	PLSR	CR	8	0.14	3.5807	0.71	3.3550
		SG	10	0.19	4.0947	0.88	4.2456
		WT	**16**	**0.20**	**4.0296**	**0.82**	**4.2045**
	SVM	CR		0.12	3.2608	0.50	3.2919
		SG		-0.25	4.1566	0.65	4.1902
		WT		-0.05	4.0916	0.69	4.1543
Piedmont/ Upper Coastal Plain	PLSR	CR	8	0.15	3.2444	0.86	3.6987
		SG	**9**	**0.62**	**4.4332**	**0.95**	**4.1822**
		WT	6	0.05	4.0744	0.92	4.2080
	SVM	CR		-0.33	3.2437	0.69	3.2990
		SG		0.09	4.1365	0.61	4.1121
		WT		-0.11	4.1088	0.79	4.1604
Coastal Plain	PLSR	CR	**10**	**0.54**	**3.2502**	**0.91**	**3.3460**
		SG	4	0.14	4.1368	0.96	4.2531
		WT	12	0.08	4.9416	0.89	4.2060
	SVM	CR		0.20	3.2839	0.60	3.3460
		SG		0.01	4.1803	0.72	4.2075
		WT		0.09	4.1501	0.67	4.1862

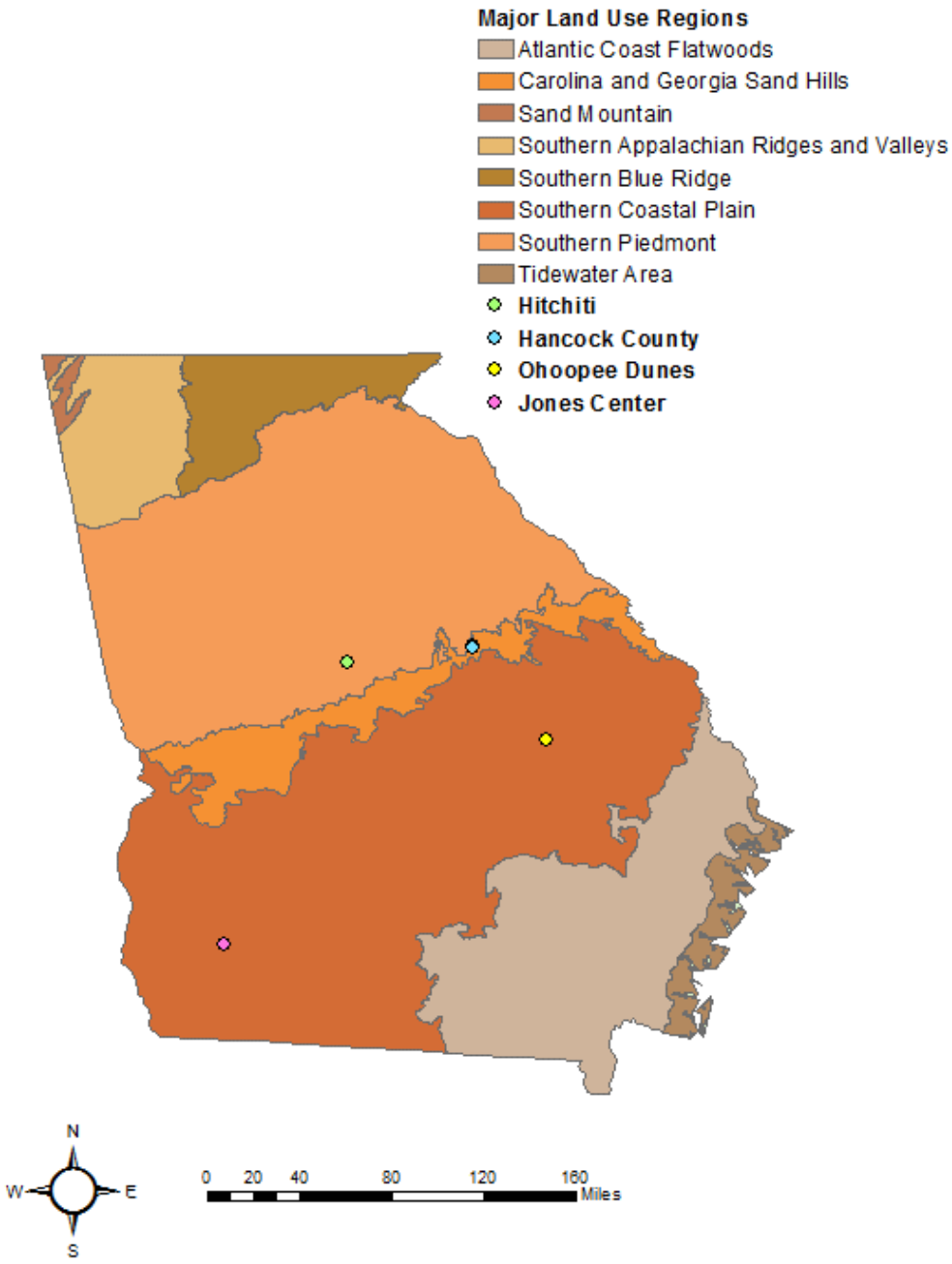

Figure 3.1: Study site locations and physiographic regions in Georgia.

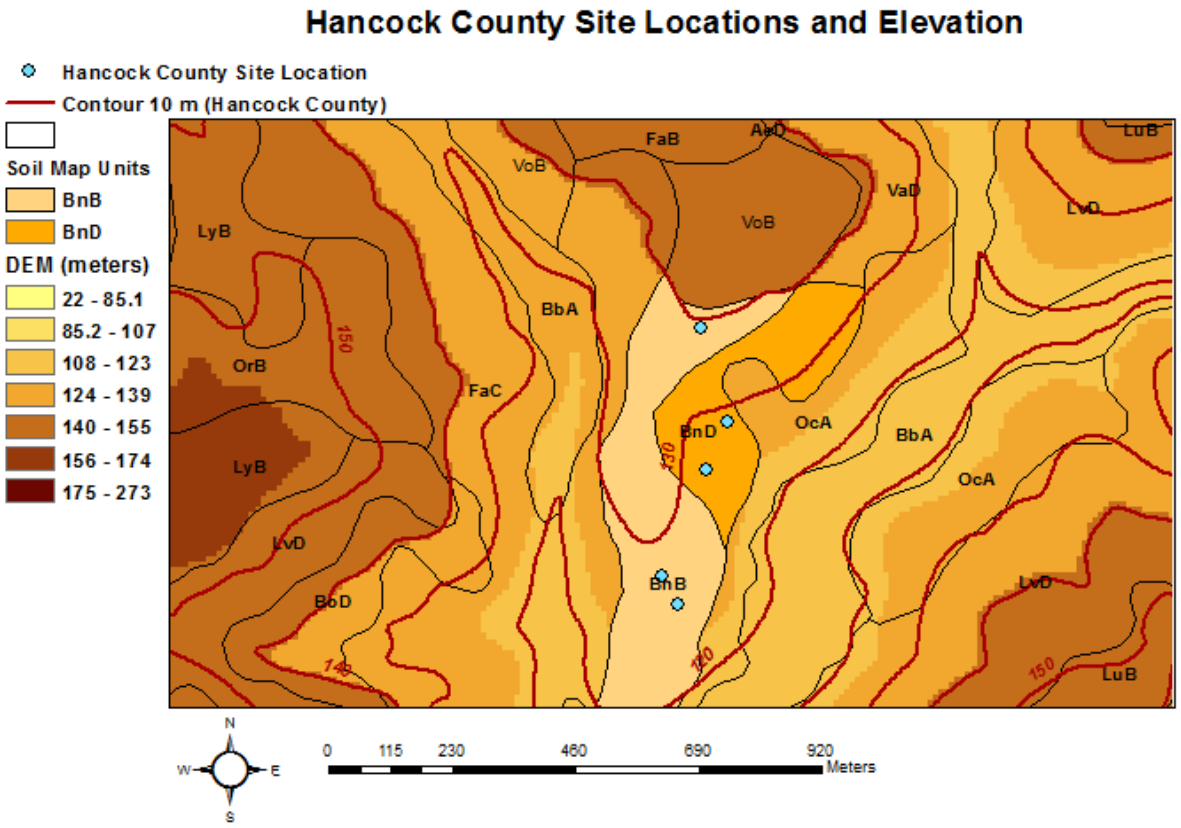

Figure 3.2: Site location and elevations within the Hancock County site in Hancock County, GA. Location points are in blue, while elevation contours are in red at 10 m intervals.

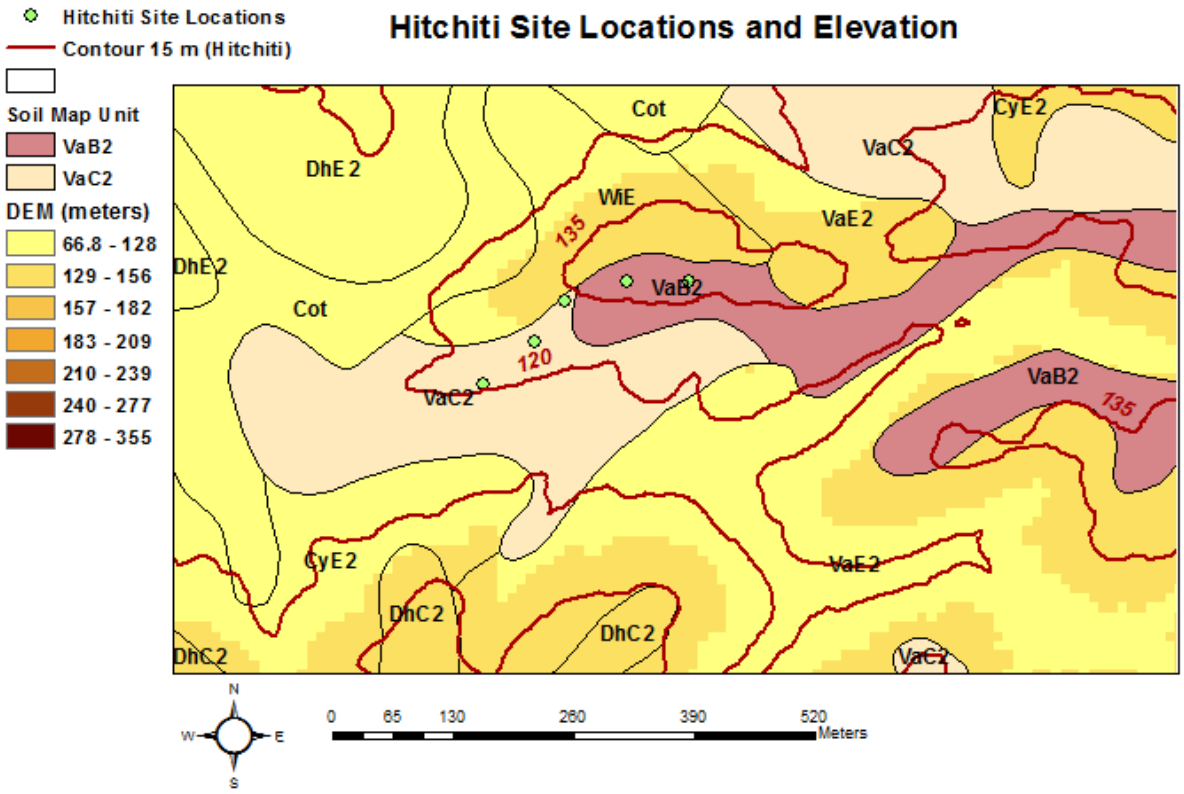

Figure 3.3: Site location and elevations within the Hitchiti site in the Oconee National Forest in Gray, GA. Location points are in green, while elevation contours are in red at 15 m intervals.

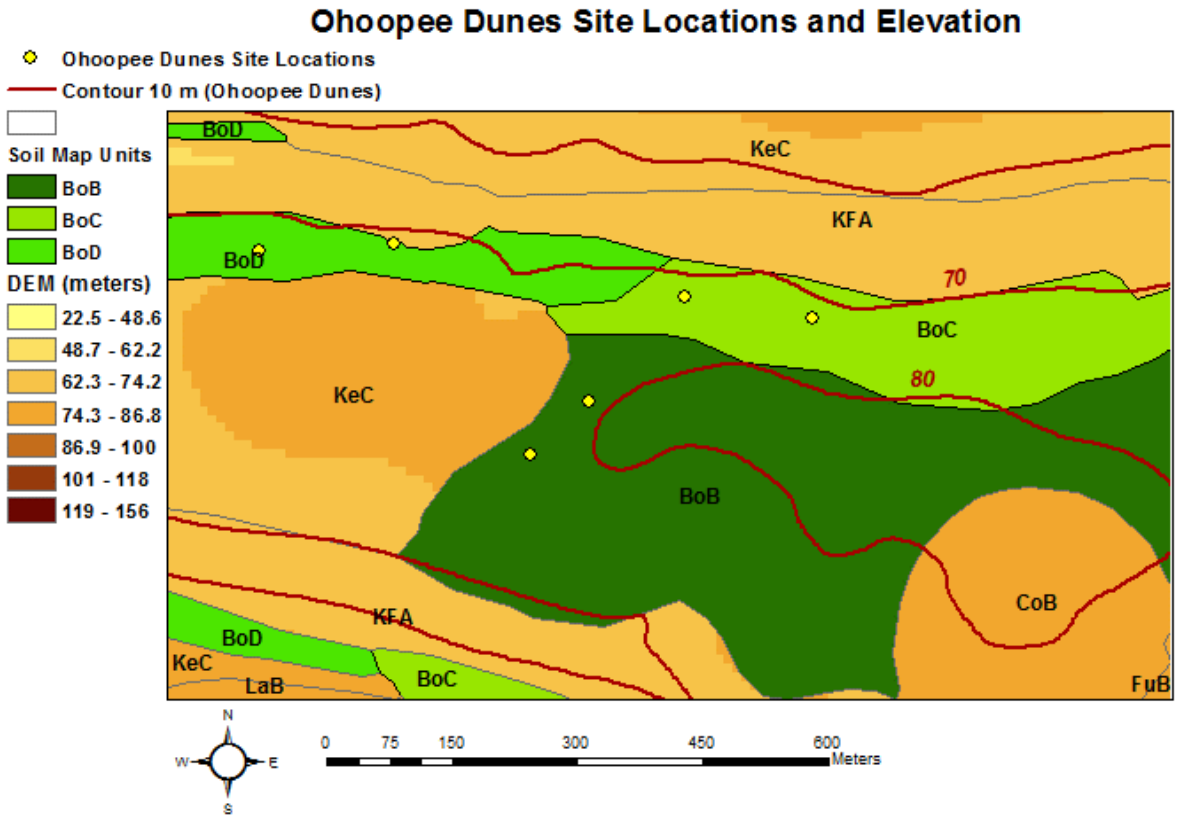

Figure 3.4: Site location and elevations within the Ohoopee Dunes Site in Swainsboro, GA. Location points are in yellow, while elevation contours are in red at 10 m intervals.

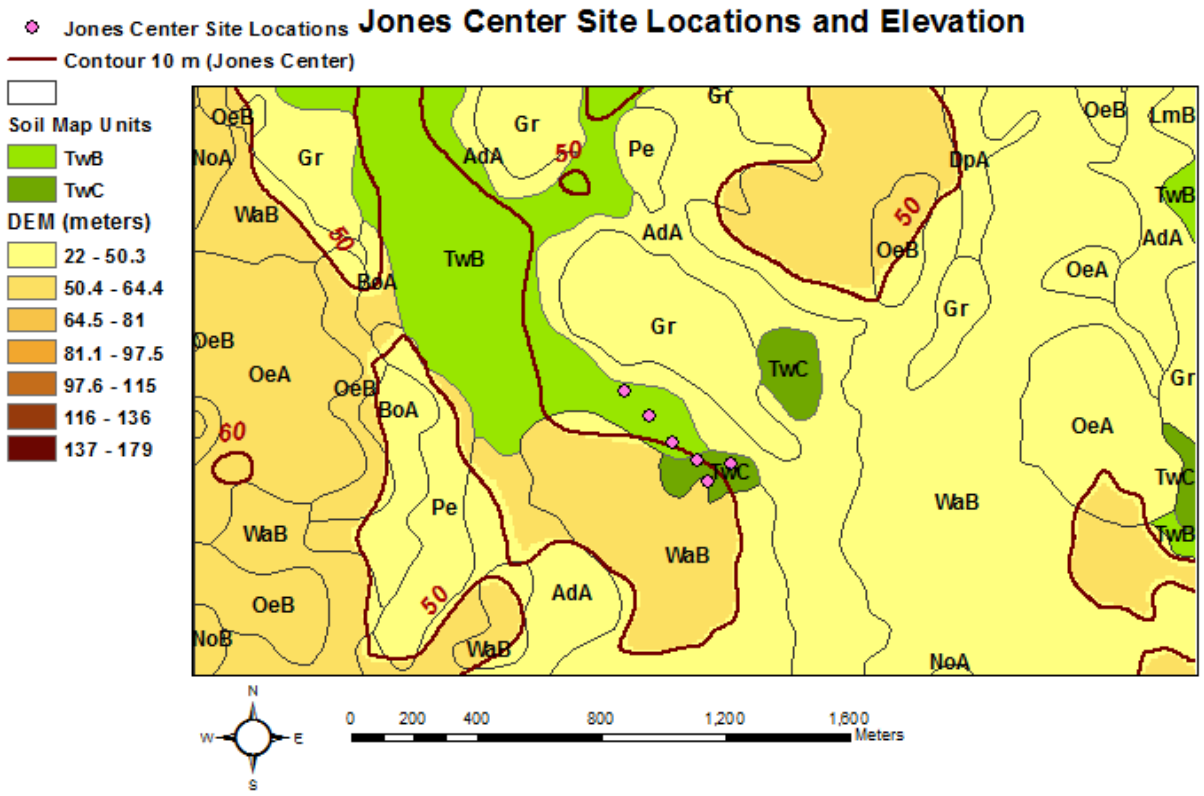

Figure 3.5: Site location and elevations within the Jones Center site in the Newton, GA. Location points are in pink, while elevation contours are in red at 10 m intervals.

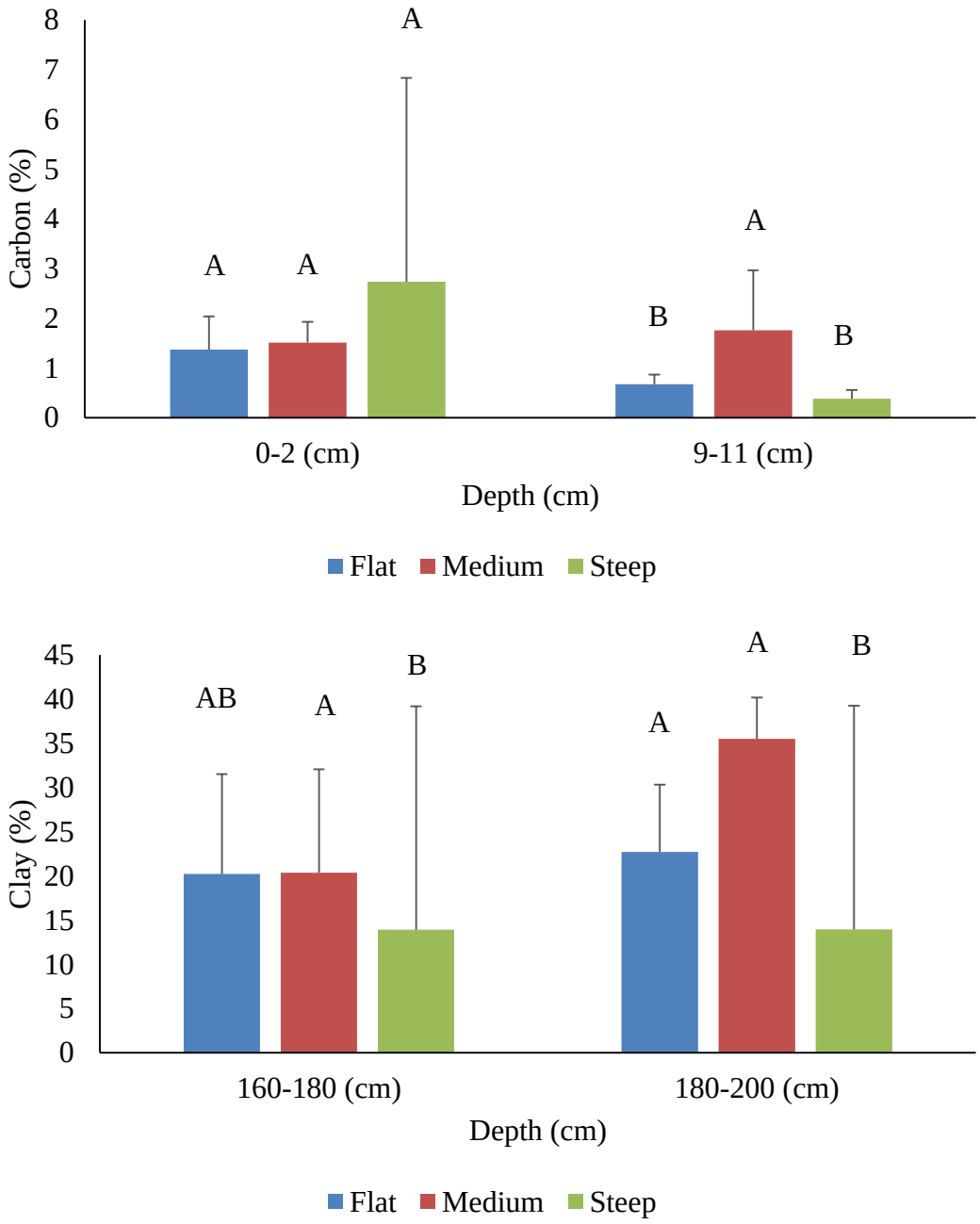

Figure 3.6: Percent carbon (top) and percent clay (bottom) averaged by depth and compared by slope (Flat, Medium, and Steep) (mean ± SD). Capital letters indicate significance among slope types and depth (Percent C: n_{Flat} = 10, n_{Medium} = 5, and n_{Steep}= 7 for each depth; Percent Clay (160-180 cm): n_{Flat} = 10, n_{Medium} = 5, and n_{Steep}= 7; Percent Clay (180-200 cm): n_{Flat} = 7, n_{Medium} = 2, and n_{Steep}= 7)

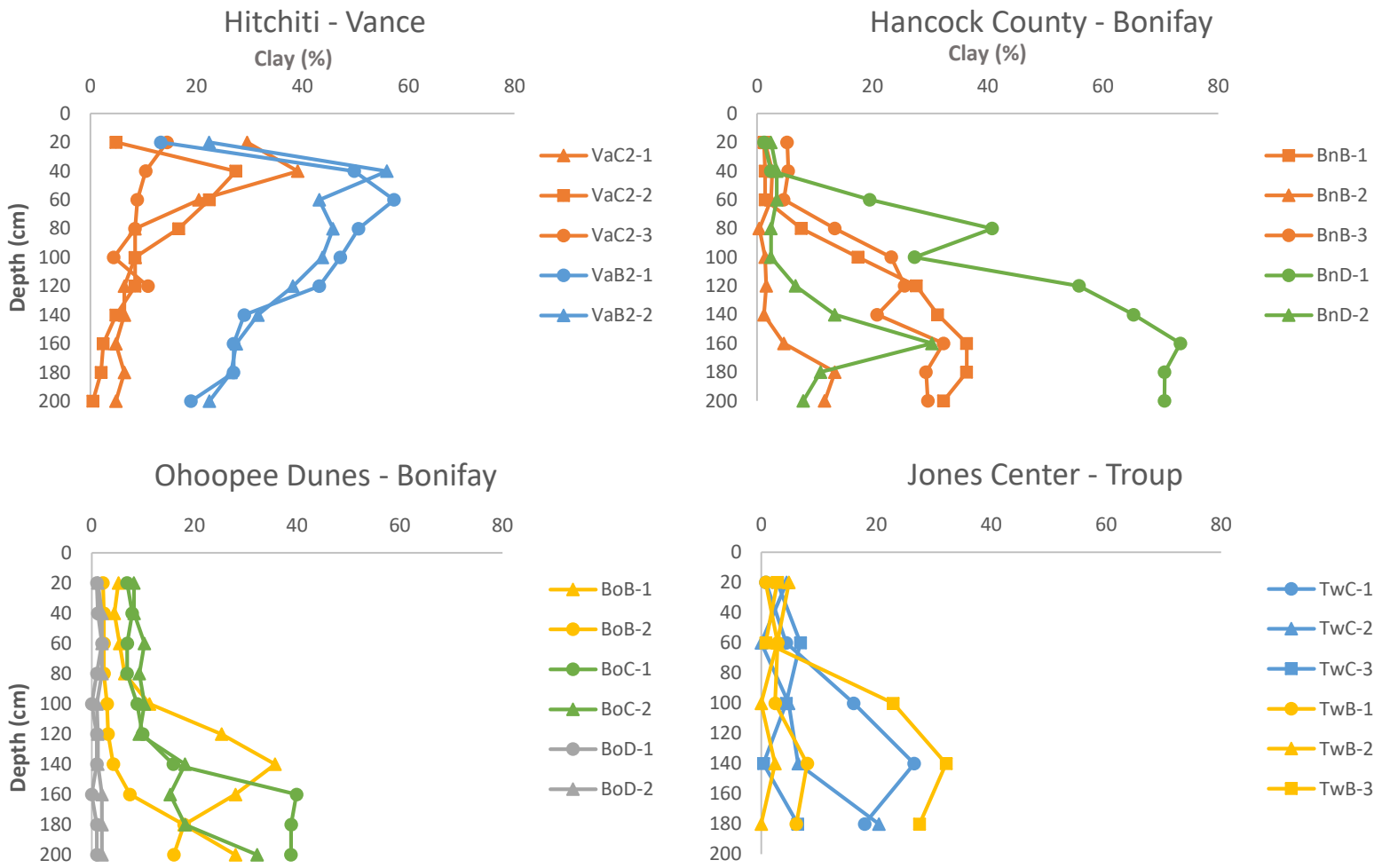

Figure 3.7: Percent clay for each site by depth and map unit soil series. Within each graph, the same color indicates the same map unit and different shape indicates different soil profile within that map unit category. Collected 2015/2016.

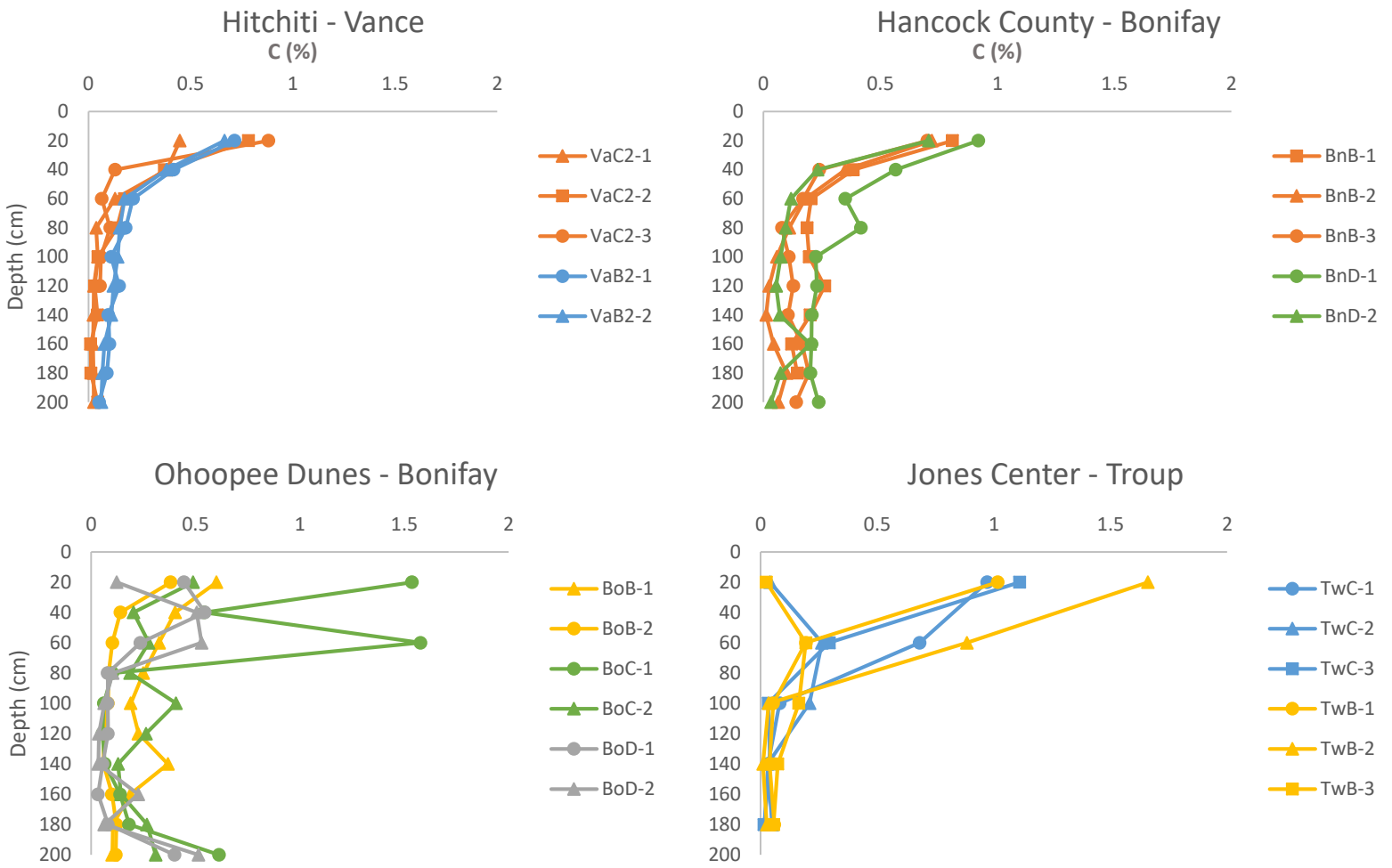

Figure 3.8: Percent C for each site by depth and map unit soil series. Within each graph, the same color indicates the same map unit and different shape indicates different soil profile within that map unit category. Collected 2015/2016.

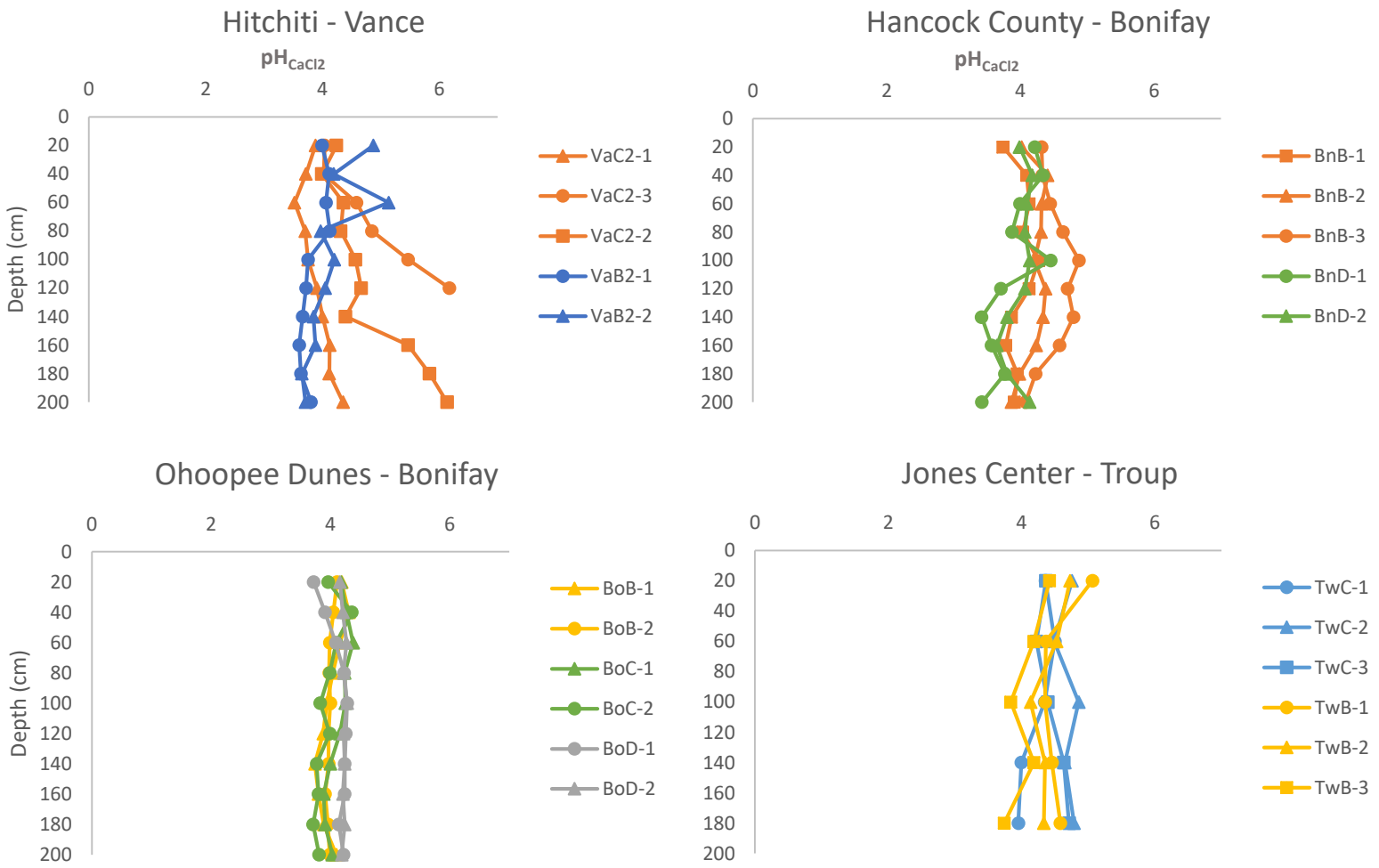

Figure 3.9: Values of pH_{CaCl2} for each site by depth and map unit soil series. Within each graph, the same color indicates the same map unit and different shape indicates different soil profile within that map unit category. Collected 2015/2016.

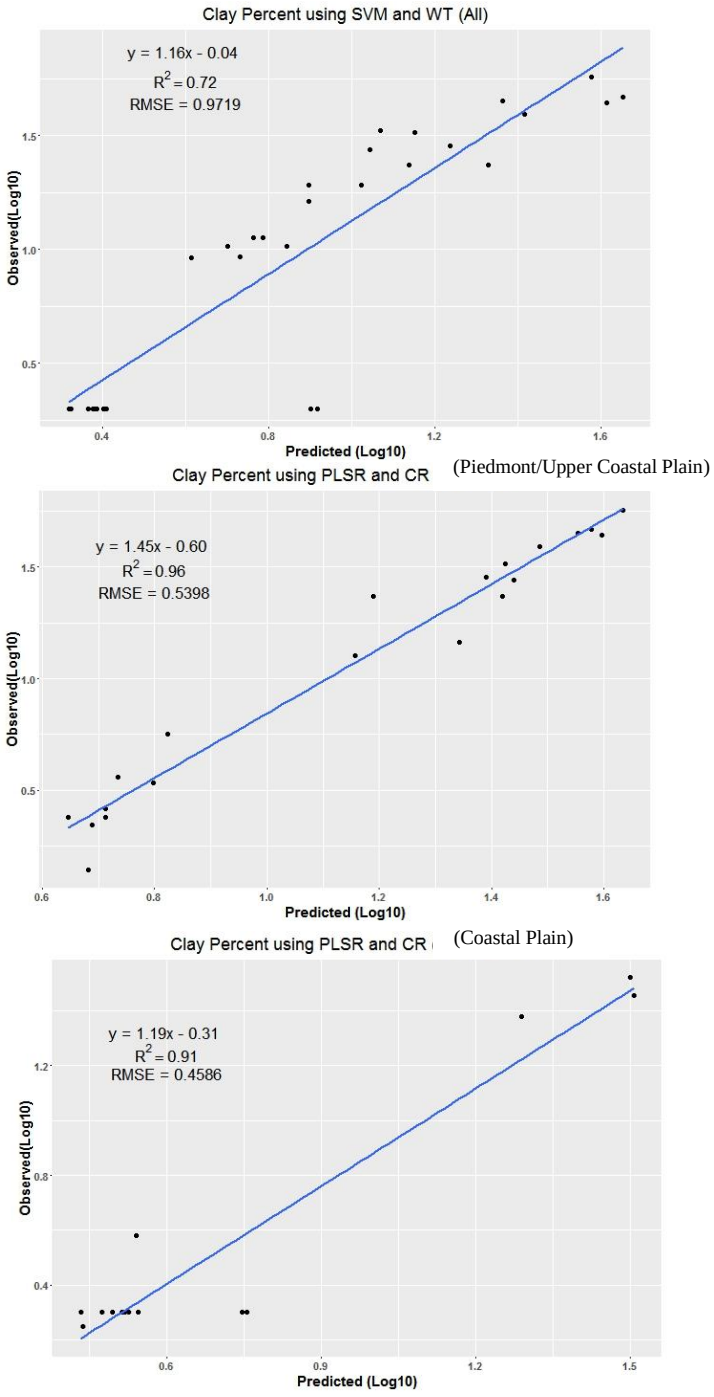

Figure 3.10: Most accurate validation scatter plot of percent clay measured vs. predicted for all clay data, Piedmont/Upper Coastal Plain data and Coastal Plain data from the four study sites. Produced from partial least square regression (PLSR) or support vector machine (SVM) with wavelets (WT) or continuum removal (CR) transformations.

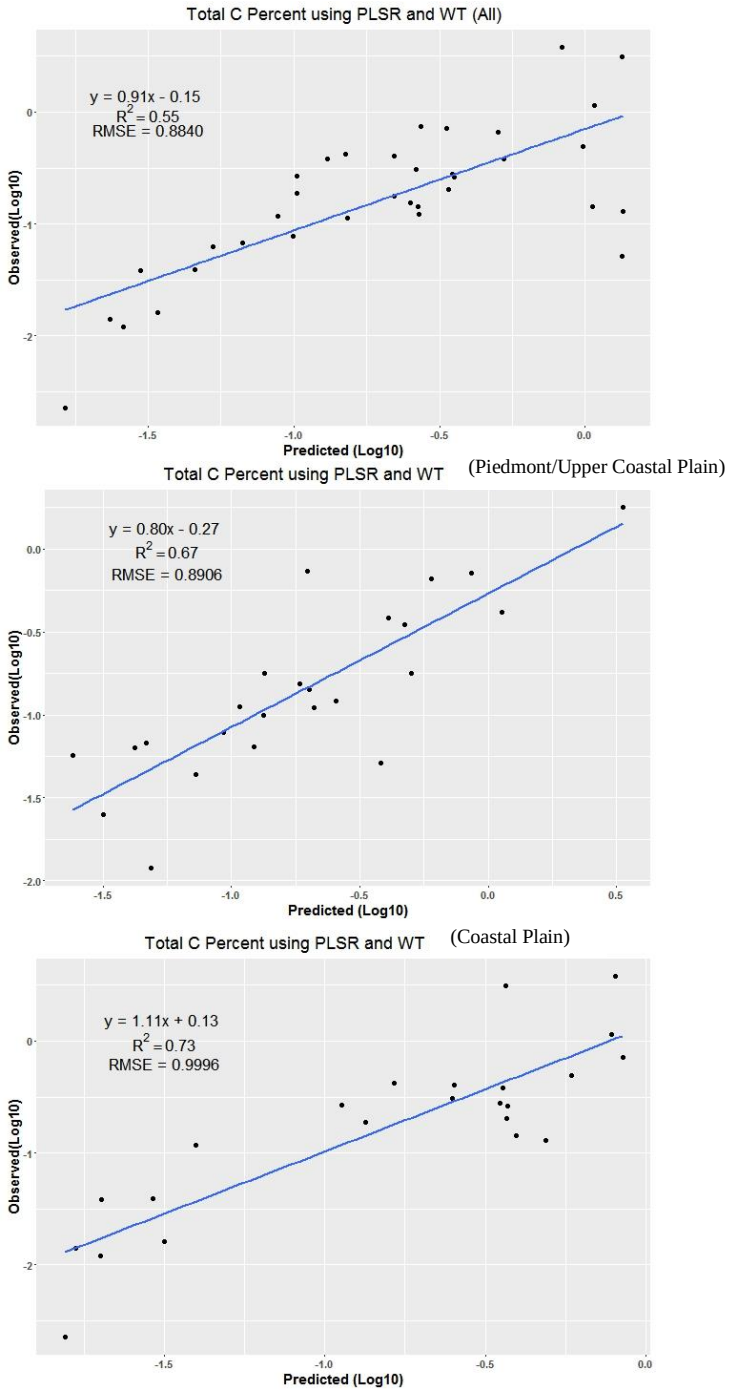

Figure 3.11: Most accurate validation scatter plot of percent C measured vs. predicted for all C data, Piedmont/Upper Coastal Plain data and Coastal Plain data from the four study sites. Produced from partial least square regression (PLSR) with wavelets (WT) or continuum removal (CR) transformations.

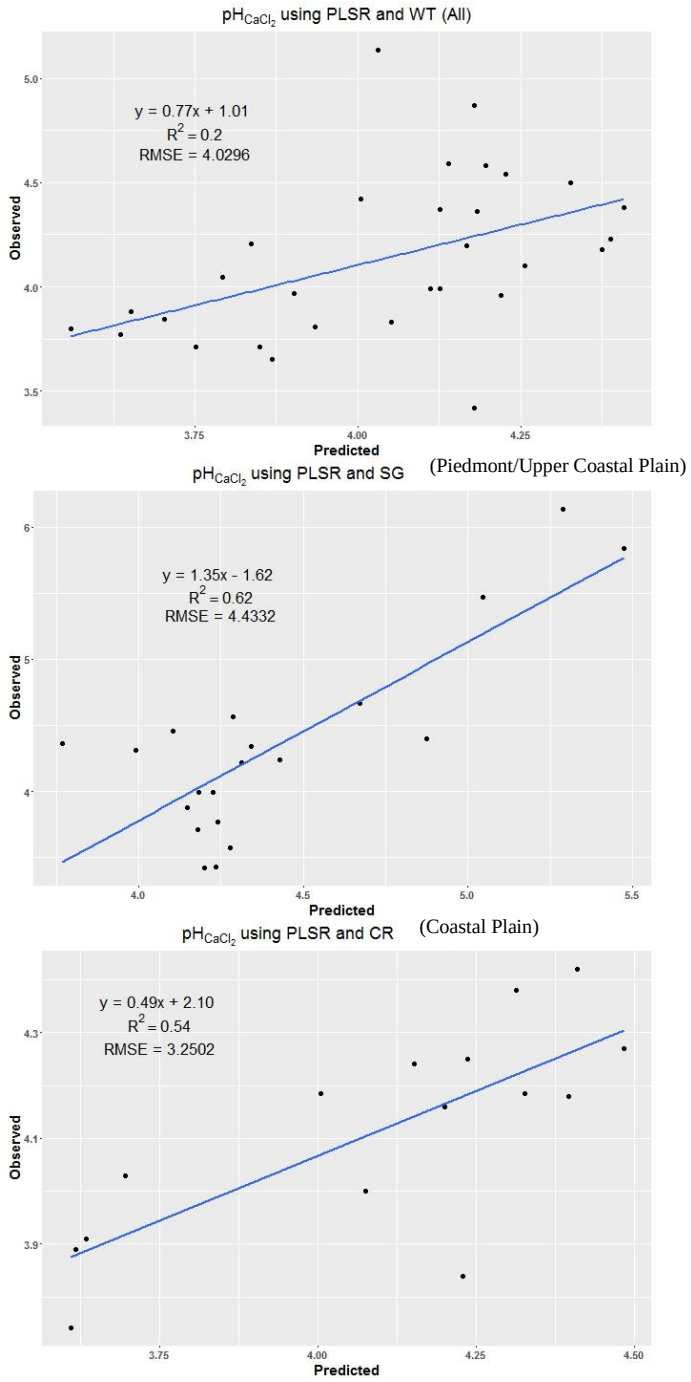

Figure 3.12: Most accurate validation scatter plot of pH_{CaCl2} measured vs. predicted for all pH_{CaCl2} data, Piedmont/Upper Coastal Plain data and Coastal Plain data from the four study sites. Produced from partial least square regression (PLSR) with wavelets (WT), Savitzky-Golay (SG), or continuum removal (CR) transformations.

CHAPTER IV

CONCLUSION

I investigated soil attributes under longleaf pine ecosystems, an ecosystem of current conservation concern. In Chapter 2 of this thesis, I evaluated multivariate calibration techniques for Visible/near-infrared (VNIR) scans to predict soil C under longleaf pine. In Chapter 3, I conducted field-based research on soil maps units (phases) under longleaf pine. Below I summarize my main findings.

Visible/near-infrared (VNIR) scanning can offer a cost effective and rapid means for capturing soil total carbon and other dynamic soil properties (DSP) in the field to evaluate management and restoration effects on soils in longleaf pine ecosystems. The geographic area covered by longleaf pine plantations is expansive and given this ecological breadth, VNIR calibrations need to be robust across multiple soil series. Data from the RaCA database and from Strickland et al. (2015), were combined to produce a sample size of 931 measured soil samples. A coefficient of determination of 70% using the support vector machine combined with the Savitzky-Golay transformation was found for soils with 0 -2 % C (mineral soil). While this multivariate calibration model still needs further development for accurate prediction of soil total C, the current model could serve as a useful tool in estimating horizontal or vertical spatial variance.

I also investigated soil map units that vary in degree of slope to determine the importance of including slope when monitoring changes in DSPs during longleaf pine

regeneration or restoration. The DSPs of interest were soil total C, clay, and pH_{CaCl2}. Results suggest that soil map unit phases capturing slope are not useful as a stratification variable for analyzing DSPs under longleaf pine restoration. Few significant differences were observed with slope steepness at any depth (0-200 cm) for the measured variables (percent clay, C, pH_{CaCl2}) and even in cases of observed differences there was not a clear monotonic pattern from flat to steep. Use of Visible/near-infrared spectroscopy was incorporated into this field study in hopes that these methods would help evaluate soil variability across slope steepness or DSPs over time. VNIR calibrations for percent clay demonstrated potential predictive value (i.e., $R^2 \geq 0.9$). While those for total soil C and pH, although not as strong, indicated some utility for field classification or monitoring of DSP, much like the total soil C models produced in Chapter 2.

Thus, VNIR calibrations can, at present, be effective currently for predicting clay percentage and also for assessing patterns of soil total C and pH_{CaCl2} across landscapes. Further development of VNIR will be valuable in facilitating the collection of more spatially explicit data at a faster rate without the need to have samples analyzed by a laboratory. With greater spatial soil data, patterns and processes in soil attributes can be better analyzed and interpreted in longleaf pine ecosystems as restoration and regeneration efforts expand.

APPENDIX A: Chapter III Supplemental Tables and Figures

Table S3.1: Prediction results of validation and cross-validation RMSE and R^2 for each data separation, method, and transformation combination for Nitrogen %, separated by all data, Piedmont/Upper Coastal Plain sites, and Coastal Plain sites. Methods: Partial Least Square Regression (PLSR) and Support Vector Machine (SVM). Transformations: Continuum Removal (CR), Savitzky-Golay (SG), and Wavelets (WT). (n_{All} = 278, $n_{Piedmont/Upper\ Coastal\ Plain}$ = 140, $n_{CoastalPlain}$= 137) Bold numbers highlight the best model result.

			Validation		Cross-Validation	
Data	**Method**	**Transformation**	**R^2**	**RMSE**	**R^2**	**RMSE**
All	PLSR	CR	0.36	2.6786	0.69	2.6174
		SG	0.14	1.7854	0.83	1.7340
		WT	**0.46**	**1.7004**	**0.75**	**1.7248**
	SVM	CR	0.10	2.6731	0.54	2.6330
		SG	0.23	1.7531	0.73	1.7416
		WT	0.40	1.7927	0.71	1.7380
Piedmont/ Upper Coastal Plain	PLSR	CR	0.17	2.6314	0.93	2.5682
		SG	**0.54**	**1.9156**	**0.94**	**1.6855**
		WT	0.33	1.5824	0.95	1.6980
	SVM	CR	-0.28	2.5760	0.71	2.5866
		SG	0.38	1.6497	0.83	1.6983
		WT	0.00	1.7000	0.89	1.7025
Coastal Plain	PLSR	CR	**0.41**	**2.6863**	**0.76**	**2.6725**
		SG	0.17	1.9170	0.94	1.7854
		WT	0.22	1.7533	0.80	1.7730
	SVM	CR	0.17	2.7674	0.59	2.6989
		SG	0.18	1.8214	0.69	1.7956
		WT	0.27	1.8445	0.67	1.7870

Table S3.2: Prediction results of validation and cross-validation RMSE and R^2 for each data separation, method, and transformation combination for Exchangeable Acidity (EA), separated by all data, Piedmont/Upper Coastal Plain sites, and Coastal Plain sites. Methods: Partial Least Square Regression (PLSR) and Support Vector Machine (SVM). Transformations: Continuum Removal (CR), Savitzky-Golay (SG), and Wavelets (WT). (n_{All} = 278, $n_{Piedmont/Upper\ Coastal\ Plain}$ = 140, $n_{CoastalPlain}$= 137) Bold numbers highlight the best model result.

			Validation		Cross-Validation	
Data	**Method**	**Transformation**	**R^2**	**RMSE**	**R^2**	**RMSE**
All	PLSR	CR	**0.43**	**1.0622**	**0.78**	**1.2058**
		SG	0.40	0.5560	0.84	0.5602
		WT	0.39	0.5666	0.77	0.5343
	SVM	CR	0.28	1.0168	0.67	1.1371
		SG	0.22	0.3944	0.78	0.4749
		WT	0.22	0.4047	0.78	0.4721
Piedmont/ Upper Coastal Plain	PLSR	CR	0.31	0.9936	0.88	1.0950
		SG	**0.47**	**0.4827**	**0.94**	**0.6093**
		WT	0.19	0.4616	0.90	0.6159
	SVM	CR	0.00	0.7906	0.74	0.9840
		SG	0.06	0.3959	0.83	0.5011
		WT	0.16	0.3533	0.84	0.5173
Coastal Plain	PLSR	CR	0.54	1.3652	0.74	1.3390
		SG	0.29	0.5005	0.88	0.5517
		WT	**0.55**	**0.4621**	**0.75**	**0.5291**
	SVM	CR	0.42	1.3182	0.49	1.2960
		SG	0.30	0.4099	0.60	0.4618
		WT	0.15	0.4061	0.60	0.4589

Table S3.3: Soil nutrients by depth within the Hancock County site located in Hancock County, Georgia. (BDL= Below Detection Limit)

		Hancock County (mg/kg)													
Sample Name	**Depth (cm)**	**Ca**	**Cd**	**Cr**	**Cu**	**Fe**	**K**	**Mg**	**Mn**	**Mo**	**Na**	**Ni**	**P**	**Pb**	**Zn**
BnD1k	0-2	174.76	BDL	0.19	0.65	25.07	108.31	620.60	1.24	BDL	21.69	0.14	1.30	BDL	0.38
BnD1L	9-11	761.77	BDL	BDL	BDL	9.81	92.91	118.02	67.19	BDL	4.72	0.72	5.91	BDL	2.94
BnD1a	0-20	215.06	BDL	BDL	BDL	5.69	10.28	20.80	8.76	BDL	BDL	0.07	1.07	BDL	0.31
BnD1b	20-40	134.52	BDL	BDL	BDL	12.59	6.46	17.94	8.55	BDL	BDL	0.07	1.14	BDL	BDL
BnD1c	40-60	574.29	BDL	0.05	BDL	9.43	7.26	164.73	2.50	BDL	6.58	BDL	0.21	BDL	BDL
BnD1d	60-80	739.62	BDL	0.06	0.31	17.63	28.45	404.33	4.98	BDL	13.66	0.07	0.30	BDL	BDL
BnD1e	80-100	310.84	BDL	0.05	BDL	11.47	16.99	146.31	2.97	BDL	7.15	0.05	0.24	BDL	BDL
BnD1f	100-120	218.75	BDL	0.11	0.21	15.41	30.86	337.12	1.60	BDL	13.54	0.06	0.24	BDL	BDL
BnD1g	120-140	431.83	BDL	0.18	0.64	20.94	87.78	605.28	3.70	BDL	22.37	0.09	0.32	BDL	0.37
BnD1h	140-160	382.30	0.04	0.30	1.08	40.77	141.37	874.23	2.73	BDL	40.49	0.07	0.89	0.08	0.46
BnD1i	160-180	293.10	0.06	0.25	1.00	31.70	169.78	979.01	2.71	BDL	35.78	0.17	0.82	BDL	0.56
BnD1j	180-200	174.76	BDL	0.19	0.65	25.07	108.31	620.60	1.24	BDL	21.69	0.14	1.30	BDL	0.38
BnD2k	0-2	241.45	BDL	BDL	0.35	63.90	31.18	19.10	59.74	BDL	8.15	0.48	6.50	BDL	2.68
BnD2L	9-11	19.79	BDL	0.08	BDL	19.17	4.43	2.69	17.88	BDL	BDL	0.13	4.67	BDL	0.23
BnD2a	0-20	45.92	0.06	0.15	0.35	37.31	10.83	5.40	30.53	BDL	7.85	0.14	8.46	0.17	0.44
BnD2b	20-40	14.39	BDL	0.05	BDL	22.56	4.34	2.80	7.75	BDL	3.90	BDL	6.36	BDL	BDL
BnD2c	40-60	13.72	BDL	0.05	0.40	30.40	22.66	3.77	5.33	BDL	6.62	BDL	8.77	BDL	0.44
BnD2d	60-80	51.43	BDL	0.05	0.30	16.89	7.87	4.35	1.10	BDL	77.59	0.07	4.32	BDL	0.99
BnD2e	80-100	36.88	BDL	0.14	0.20	43.68	7.70	9.07	1.37	BDL	4.85	BDL	6.41	BDL	0.39
BND2F	100-120	31.54	BDL	BDL	BDL	13.79	3.36	9.29	0.21	BDL	2.14	BDL	1.32	BDL	BDL
BnD2g	120-140	18.00	BDL	0.06	BDL	10.21	4.98	9.63	0.20	BDL	BDL	BDL	0.35	BDL	BDL
BnD2h	140-160	40.73	BDL	0.20	0.32	25.51	8.36	26.86	1.54	BDL	8.35	BDL	0.72	BDL	BDL
BnD2i	160-180	11.08	BDL	BDL	BDL	4.48	2.61	6.86	BDL	BDL	BDL	BDL	0.34	BDL	BDL
BnD2j	180-200	11.57	BDL	BDL	BDL	4.49	BDL	6.83	BDL	BDL	3.58	0.05	0.85	BDL	BDL
BnB1k	0-2	206.70	BDL	BDL	BDL	16.81	18.69	19.82	24.35	BDL	BDL	0.27	2.00	BDL	1.00
BnB1L	9-11	87.15	BDL	BDL	BDL	14.83	15.00	12.38	8.70	BDL	2.50	0.34	1.74	BDL	0.46

BnB1a	0-20	19.74	BDL	BDL	BDL	7.00	6.39	4.18	2.79	BDL	3.15	BDL	0.49	BDL	BDL
BnB1b	20-40	10.70	BDL	0.05	BDL	5.77	4.04	2.29	4.80	BDL	BDL	BDL	0.68	BDL	BDL
BnB1c	40-60	7.74	BDL	BDL	BDL	7.34	3.85	2.77	2.66	BDL	BDL	BDL	0.49	BDL	BDL
BnB1d	60-80	12.23	BDL	BDL	BDL	4.99	4.40	8.21	1.59	BDL	BDL	BDL	0.17	BDL	BDL
BnB1e	80-100	117.56	BDL	BDL	BDL	6.54	10.96	32.01	1.61	BDL	BDL	BDL	0.24	BDL	BDL
BnB1f	100-120	87.15	BDL	BDL	BDL	1.49	8.43	25.53	0.35	BDL	BDL	BDL	BDL	BDL	BDL
BnB1g	120-140	33.36	BDL	BDL	BDL	6.32	3.73	26.51	1.23	BDL	BDL	BDL	0.12	BDL	BDL
BnB1h	140-160	9.60	BDL	BDL	BDL	4.01	2.41	14.77	0.32	BDL	BDL	BDL	0.08	BDL	BDL
BnB1i	160-180	4.13	BDL	BDL	BDL	1.56	BDL	8.71	BDL	BDL	BDL	BDL	BDL	BDL	BDL
BnB1j	180-200	6.88	BDL	BDL	BDL	2.98	3.44	14.80	0.22	BDL	2.44	BDL	0.12	BDL	BDL
BnB2k	0-2	76.70	BDL	BDL	BDL	48.89	8.63	11.18	16.02	BDL	BDL	0.12	5.23	BDL	0.67
BnB2L	9-11	6.13	BDL	0.09	BDL	66.05	3.79	1.38	15.46	BDL	BDL	0.22	42.81	0.10	BDL
BnB2a	0-20	30.20	BDL	0.05	BDL	56.93	6.97	3.61	18.03	BDL	2.73	0.27	22.39	BDL	0.31
BnB2b	20-40	15.18	BDL	0.10	BDL	84.73	8.26	3.81	24.31	BDL	6.08	0.05	23.22	BDL	0.26
BnB2c	40-60	27.29	BDL	0.05	BDL	45.15	4.32	6.43	12.38	BDL	2.65	BDL	15.92	BDL	BDL
BnB2d	60-80	15.46	BDL	BDL	BDL	20.02	4.02	3.53	9.92	BDL	BDL	BDL	5.43	BDL	BDL
BnB2e	80-100	14.80	BDL	BDL	BDL	16.09	2.24	3.55	2.69	BDL	BDL	BDL	3.92	BDL	BDL
BnB2f	100-120	19.31	BDL	0.07	BDL	47.68	9.02	5.89	1.76	BDL	4.17	0.05	4.98	BDL	BDL
BnB2g	120-140	22.49	BDL	BDL	BDL	16.56	6.00	3.15	1.20	BDL	2.83	BDL	4.03	BDL	BDL
BnB2h	140-160	76.00	BDL	BDL	BDL	34.90	9.75	11.13	1.26	BDL	4.24	BDL	10.63	BDL	BDL
BnB2i	160-180	148.93	BDL	0.13	0.20	50.47	18.01	29.07	1.47	BDL	5.36	BDL	5.74	BDL	BDL
BnB2j	180-200	59.62	BDL	0.06	BDL	20.29	9.35	15.87	1.67	BDL	4.34	BDL	2.06	BDL	BDL
BnB3k	0-2	805.72	0.06	BDL	0.22	24.62	81.43	86.39	57.49	BDL	4.58	0.51	5.39	BDL	2.57
BnB3L	9-11	58.77	BDL	0.06	BDL	18.33	9.72	15.33	24.54	BDL	BDL	0.13	1.99	BDL	0.26
BnB3a	0-20	44.07	BDL	BDL	BDL	10.44	8.45	6.49	9.47	BDL	BDL	BDL	0.86	BDL	BDL
BnB3b	20-40	49.56	BDL	BDL	0.21	16.69	8.99	11.42	8.24	BDL	3.79	0.05	1.63	BDL	BDL
BnB3c	40-60	37.64	BDL	BDL	BDL	5.12	5.04	5.50	2.76	BDL	BDL	BDL	0.98	BDL	BDL
BnB3d	60-80	145.46	BDL	BDL	BDL	5.86	7.86	23.82	0.56	BDL	BDL	BDL	0.30	BDL	BDL
BnB3e	80-100	195.21	BDL	BDL	BDL	3.53	5.47	41.63	0.22	BDL	BDL	BDL	0.09	BDL	BDL
BnB3f	100-120	185.91	BDL	BDL	BDL	5.84	10.97	115.89	0.52	BDL	5.90	BDL	0.16	BDL	BDL
BnB3g	120-140	450.98	BDL	BDL	0.21	10.76	20.99	152.90	0.99	BDL	9.33	BDL	0.70	BDL	BDL
BnB3h	140-160	347.58	BDL	BDL	BDL	4.52	10.03	132.71	0.25	BDL	4.57	BDL	0.09	BDL	BDL
BnB3i	160-180	399.36	BDL	BDL	0.31	14.34	15.97	213.88	0.38	BDL	9.65	BDL	0.18	BDL	BDL
BnB3j	180-200	174.67	BDL	BDL	0.24	11.98	8.74	114.08	0.42	BDL	5.09	BDL	0.22	BDL	BDL

Table S3.4: Soil nutrients by depth within the Hitchiti Experimental Forest site located near Juliet, Georgia. (BDL= Below Detection Limit)

Hitchiti Experimental Forest (mg/kg)															
Sample Name	**Depth (cm)**	**Ca**	**Cd**	**Cr**	**Cu**	**Fe**	**K**	**Mg**	**Mn**	**Mo**	**Na**	**Ni**	**P**	**Pb**	**Zn**
VaB2-1k	0-2	112.20	BDL	BDL	0.51	44.52	19.42	19.07	14.22	BDL	BDL	0.19	1.14	BDL	0.99
VaB2-1L	9-11	96.20	BDL	0.06	0.57	24.92	26.57	93.47	4.32	BDL	BDL	0.11	0.39	BDL	0.34
VaB2-1a	0-20	16.11	BDL	BDL	BDL	10.76	7.19	7.85	4.23	BDL	BDL	BDL	0.22	BDL	0.24
VaB2-1b	20-40	81.82	BDL	BDL	0.61	13.65	40.43	229.39	4.62	BDL	9.08	BDL	0.34	BDL	0.54
VaB2-1c	40-60	14.96	BDL	BDL	0.30	7.97	14.69	108.07	BDL	BDL	6.89	BDL	0.16	BDL	BDL
VaB2-1d	60-80	8.76	BDL	BDL	0.58	15.61	11.46	176.19	BDL	BDL	14.26	BDL	0.25	BDL	BDL
VaB2-1e	80-100	BDL	BDL	BDL	0.24	7.60	BDL	63.74	BDL	BDL	8.37	BDL	BDL	BDL	BDL
VaB2-1f	100-120	2.16	BDL	BDL	0.26	9.43	BDL	44.53	BDL	BDL	12.43	BDL	0.15	BDL	BDL
VaB2-1g	120-140	4.83	BDL	BDL	0.51	19.38	5.81	93.63	BDL	BDL	44.90	0.06	0.24	BDL	BDL
VaB2-1h	140-160	3.30	BDL	BDL	0.35	10.78	2.81	43.77	BDL	BDL	36.61	BDL	0.18	BDL	BDL
VaB2-1i	160-180	5.51	BDL	BDL	0.75	20.70	9.41	65.27	BDL	BDL	78.70	BDL	0.28	BDL	0.32
VaB2-1j	180-200	4.02	BDL	BDL	0.42	8.37	4.33	43.28	BDL	BDL	58.82	BDL	0.30	BDL	BDL
VaB2-2k	0-2	573.54	BDL	BDL	BDL	13.35	29.49	53.52	20.29	BDL	BDL	0.15	1.15	BDL	2.15
VaB2-2L	9-11	189.76	BDL	BDL	0.23	36.85	27.62	50.75	8.14	BDL	BDL	0.13	0.46	BDL	0.25
VaB2-2a	0-20	306.34	BDL	BDL	0.79	20.69	102.15	138.93	16.63	BDL	6.61	0.07	1.26	BDL	1.18
VaB2-2b	20-40	259.27	BDL	BDL	0.33	9.46	43.35	181.10	0.46	BDL	6.49	0.04	0.16	BDL	BDL
VaB2-2c	40-60	116.86	BDL	BDL	0.28	9.26	22.60	156.71	BDL	BDL	10.33	BDL	0.12	BDL	BDL
VaB2-2d	60-80	60.38	BDL	BDL	BDL	9.35	18.08	135.34	BDL	BDL	14.38	BDL	0.14	BDL	BDL
VaB2-2e	80-100	79.85	BDL	BDL	0.47	23.41	38.83	374.68	0.35	BDL	66.73	0.08	0.23	BDL	0.27
VaB2-2f	100-120	14.79	BDL	BDL	BDL	8.88	9.37	149.23	BDL	BDL	37.30	BDL	BDL	BDL	BDL
VaB2-2g	120-140	9.92	BDL	BDL	BDL	7.18	4.86	173.09	0.54	BDL	60.88	BDL	0.10	BDL	BDL
VaB2-2h	140-160	11.76	BDL	BDL	0.25	14.03	4.00	249.10	1.09	BDL	102.70	0.07	BDL	BDL	0.28
VaB2-2i	160-180	20.64	BDL	BDL	0.35	19.14	5.62	417.99	1.65	BDL	175.54	0.13	0.15	BDL	0.58
VaB2-2j	180-200	26.17	BDL	BDL	0.33	12.48	3.99	325.52	0.76	BDL	167.94	0.12	0.10	BDL	0.52
VaC2-1k	0-2	280.33	BDL	0.04	0.35	62.60	37.84	104.11	19.90	BDL	4.19	0.22	1.08	BDL	0.44

VaC2-1L	9-11	205.65	BDL	BDL	1.07	39.36	19.16	205.18	1.92	BDL	19.28	0.15	0.32	BDL	BDL
VaC2-1a	0-20	217.34	BDL	0.05	0.73	53.98	33.53	164.50	8.18	BDL	14.41	BDL	0.39	BDL	0.20
VaC2-1b	20-40	284.75	BDL	0.06	1.99	64.30	35.41	519.43	1.41	BDL	57.73	0.10	0.60	BDL	0.23
VaC2-1c	40-60	204.31	BDL	BDL	1.88	51.43	50.88	890.25	0.78	BDL	152.21	0.15	0.52	BDL	BDL
VaC2-1d	60-80	27.15	BDL	BDL	0.24	6.49	6.00	115.59	BDL	BDL	24.26	BDL	BDL	BDL	BDL
VaC2-1e	80-100	48.79	BDL	BDL	0.35	9.13	9.95	151.63	0.37	BDL	38.36	BDL	0.21	BDL	BDL
VaC2-1f	100-120	101.05	BDL	BDL	0.36	8.04	14.84	232.51	0.26	BDL	57.68	0.05	0.46	BDL	BDL
VaC2-1g	120-140	126.35	BDL	BDL	0.30	5.26	7.61	188.34	BDL	BDL	52.63	0.04	0.18	BDL	BDL
VaC2-1h	140-160	155.15	BDL	BDL	0.31	5.72	7.48	201.18	BDL	BDL	66.16	0.05	0.18	BDL	0.22
VaC2-1i	160-180	168.48	BDL	BDL	0.46	10.31	14.86	266.84	0.41	BDL	97.80	0.07	0.35	BDL	0.31
VaC2-1j	180-200	158.08	BDL	BDL	0.38	11.36	12.38	204.00	0.62	BDL	96.47	0.08	0.48	BDL	0.28
VaC2-2k	0-2	602.60	0.06	BDL	0.48	52.72	185.03	141.95	58.45	BDL	18.55	1.78	6.66	BDL	5.46
VaC2-2L	9-11	26.71	BDL	BDL	BDL	13.13	7.80	12.42	9.59	BDL	BDL	0.10	0.53	BDL	0.20
VaC2-2a	0-20	161.45	BDL	BDL	0.21	41.02	20.99	35.91	12.10	BDL	6.10	0.08	0.67	BDL	0.77
VaC2-2b	20-40	224.81	BDL	BDL	0.70	25.49	11.04	206.45	6.53	BDL	19.25	0.07	0.48	BDL	0.28
VaC2-2c	40-60	295.80	BDL	BDL	0.30	17.65	4.52	276.85	0.71	BDL	45.78	BDL	0.49	BDL	BDL
VaC2-2d	60-80	522.30	BDL	BDL	0.21	20.25	3.89	574.06	1.51	BDL	109.74	0.11	0.16	BDL	0.37
VaC2-2e	80-100	375.99	BDL	BDL	BDL	20.87	5.43	490.49	2.42	BDL	128.51	0.12	0.24	BDL	0.50
VaC2-2f	100-120	369.91	BDL	BDL	BDL	11.44	4.56	462.25	1.85	BDL	186.37	0.11	0.25	BDL	0.36
VaC2-2g	120-140	173.34	BDL	BDL	BDL	19.96	9.40	305.98	4.37	BDL	149.75	0.08	0.64	BDL	0.33
VaC2-2h	140-160	347.75	BDL	BDL	BDL	43.26	17.13	475.47	29.77	BDL	253.18	0.26	4.10	BDL	0.55
VaC2-2i	160-180	446.75	BDL	BDL	BDL	27.82	9.61	198.11	18.35	BDL	128.86	0.10	83.75	BDL	0.26
VaC2-2j	180-200	468.36	BDL	BDL	0.39	69.52	26.79	275.77	73.18	BDL	191.44	0.34	81.87	BDL	1.03
VaC2-3k	0-2	442.08	BDL	BDL	0.23	19.51	35.59	185.90	14.23	BDL	10.82	0.27	1.00	BDL	0.42
VaC2-3L	9-11	116.06	BDL	BDL	BDL	13.98	12.23	153.41	0.46	BDL	12.26	0.07	0.56	BDL	BDL
VaC2-3a	0-20	455.88	BDL	BDL	0.27	21.47	27.28	224.10	8.30	BDL	13.73	BDL	1.29	BDL	0.48
VaC2-3b	20-40	472.72	BDL	BDL	0.20	19.74	14.03	395.55	1.90	BDL	42.53	BDL	91.38	BDL	BDL
VaC2-3c	40-60	919.24	BDL	BDL	0.72	33.16	30.95	1061.15	5.23	BDL	222.75	0.12	273.34	BDL	0.59
VaC2-3d	60-80	679.26	BDL	0.07	0.38	15.07	11.31	389.40	2.48	BDL	161.56	0.07	117.77	BDL	0.20
VaC2-3e	80-100	487.22	BDL	BDL	0.23	12.24	5.78	296.12	4.00	BDL	148.75	0.06	114.60	BDL	BDL
VaC2-3f	100-120	666.13	BDL	BDL	1.71	15.84	25.44	1317.96	11.28	BDL	875.80	0.22	56.39	BDL	0.66

Table S3.5: Soil nutrients by depth within the Ohoopee Dunes site located near Swainsboro, Georgia. (BDL= Below Detection Limit)

Ohoopee Dunes (mg/kg)															
Sample Name	**Depth (cm)**	**Ca**	**Cd**	**Cr**	**Cu**	**Fe**	**K**	**Mg**	**Mn**	**Mo**	**Na**	**Ni**	**P**	**Pb**	**Zn**
Bob1k	0-2	63.40	BDL	0.04	0.10	38.88	18.58	14.25	44.51	BDL	1.79	BDL	1.55	BDL	BDL
Bob1L	9-11	44.44	BDL	0.06	0.12	35.71	13.62	11.55	28.36	BDL	1.63	BDL	1.55	BDL	BDL
Bob1a	0-20	49.83	BDL	0.05	0.50	22.86	14.39	11.90	21.57	BDL	2.94	BDL	1.16	BDL	BDL
Bob1b	20-40	35.39	BDL	BDL	0.16	14.80	10.33	12.36	18.06	BDL	2.66	BDL	0.79	BDL	BDL
Bob1c	40-60	18.61	BDL	BDL	0.13	15.22	6.73	8.11	8.40	BDL	1.97	BDL	0.66	BDL	BDL
Bob1d	60-80	17.89	BDL	BDL	0.52	11.79	10.47	8.68	10.42	BDL	4.50	BDL	0.71	BDL	BDL
Bob1e	80-100	20.56	BDL	0.04	0.11	19.09	7.59	17.73	5.30	BDL	2.47	BDL	0.60	BDL	BDL
Bob1f	100-120	22.38	BDL	0.04	0.18	21.47	5.79	21.49	4.29	BDL	3.20	BDL	BDL	BDL	BDL
Bob1g	120-140	17.35	BDL	0.13	0.20	55.74	8.24	20.62	13.25	BDL	6.34	BDL	BDL	BDL	BDL
Bob1h	140-160	19.29	BDL	BDL	0.16	16.99	4.65	17.35	5.94	BDL	4.92	BDL	BDL	BDL	BDL
Bob1i	160-180	10.62	BDL	BDL	0.14	8.48	3.30	19.85	1.34	BDL	4.69	BDL	BDL	BDL	BDL
Bob1j	180-200	12.48	BDL	BDL	0.11	10.42	3.84	16.50	3.87	BDL	2.82	BDL	0.63	BDL	BDL
Bob2k	0-2	19.53	BDL	BDL	0.12	36.75	14.26	4.29	32.28	BDL	1.96	BDL	1.96	BDL	BDL
Bob2L	9-11	4.03	BDL	0.05	0.16	23.30	6.68	1.57	13.28	BDL	1.69	BDL	1.65	BDL	BDL
Bob2a	0-20	5.14	BDL	BDL	0.14	13.48	8.56	1.71	9.14	BDL	3.87	BDL	0.90	BDL	BDL
Bob2b	20-40	2.58	BDL	BDL	0.08	12.47	BDL	1.05	4.17	BDL	BDL	BDL	0.52	BDL	BDL
Bob2c	40-60	2.66	BDL	BDL	0.06	9.56	BDL	1.01	2.63	BDL	BDL	BDL	0.62	BDL	BDL
Bob2d	60-80	2.41	BDL	BDL	0.06	8.51	BDL	0.95	2.60	BDL	BDL	BDL	1.09	BDL	BDL
Bob2e	80-100	4.05	BDL	BDL	0.08	11.52	3.03	1.42	2.66	BDL	1.79	BDL	1.01	BDL	BDL
Bob2f	100-120	2.32	BDL	BDL	0.09	11.81	2.80	0.85	0.77	BDL	1.94	BDL	1.55	BDL	BDL
Bob2g	120-140	3.17	BDL	BDL	0.08	21.84	2.80	1.35	0.64	BDL	BDL	BDL	2.17	BDL	BDL
Bob2h	140-160	4.59	BDL	0.05	0.23	17.40	5.02	2.05	1.48	BDL	2.43	BDL	1.31	BDL	BDL
Bob2i	160-180	34.95	BDL	0.04	0.12	18.28	6.58	28.58	1.80	BDL	2.67	BDL	0.55	BDL	BDL

Bob2j	180-200	11.99	BDL	0.04	0.14	15.67	5.82	13.90	2.27	BDL	2.92	BDL	0.58	BDL	BDL
BoC1k	0-2	121.78	BDL	BDL	0.16	34.43	14.92	10.21	21.02	BDL	2.68	BDL	1.40	BDL	BDL
BoC1L	9-11	33.51	BDL	0.05	0.18	36.99	4.66	3.66	11.74	BDL	BDL	BDL	0.95	BDL	BDL
BoC1a	0-20	174.90	BDL	BDL	0.17	26.67	17.09	15.89	22.90	BDL	3.60	BDL	1.63	BDL	BDL
BoC1b	20-40	48.65	BDL	0.04	0.20	18.52	5.40	5.73	9.58	BDL	2.64	BDL	0.98	BDL	BDL
BoC1c	40-60	27.24	BDL	BDL	0.15	9.26	10.89	6.04	3.75	BDL	2.38	BDL	0.43	BDL	BDL
BoC1d	60-80	16.43	BDL	BDL	0.12	7.98	5.05	3.56	3.82	BDL	1.88	BDL	0.47	BDL	BDL
BoC1e	80-100	18.21	BDL	BDL	0.11	9.74	3.22	5.47	3.43	BDL	BDL	BDL	0.48	BDL	BDL
BoC1f	100-120	16.80	BDL	BDL	0.09	5.31	3.54	4.19	1.66	BDL	1.82	BDL	BDL	BDL	BDL
BoC1g	120-140	47.53	BDL	BDL	0.12	10.15	5.96	18.11	1.91	BDL	2.06	BDL	BDL	BDL	BDL
BoC1h	140-160	162.18	BDL	BDL	0.20	6.01	8.60	60.15	1.22	BDL	5.10	BDL	BDL	BDL	BDL
BoC1i	160-180	148.04	BDL	BDL	0.22	10.02	7.41	49.86	3.76	BDL	4.98	BDL	0.46	BDL	BDL
BoC1j	180-200	217.50	BDL	BDL	0.20	10.15	10.01	66.36	5.74	BDL	5.16	BDL	0.46	BDL	BDL
BoC2k	0-2	136.63	BDL	0.05	0.12	37.07	13.00	20.49	37.78	BDL	2.41	BDL	1.71	BDL	BDL
BoC2L	9-11	47.02	BDL	0.05	0.23	26.30	8.80	9.07	21.78	BDL	2.62	BDL	1.23	BDL	BDL
BoC2a	0-20	41.09	BDL	0.04	0.20	23.39	9.12	11.34	15.75	BDL	1.67	BDL	0.98	BDL	BDL
BoC2b	20-40	16.39	BDL	0.04	0.17	21.52	7.26	7.64	11.91	BDL	4.35	BDL	0.87	BDL	BDL
BoC2c	40-60	10.94	BDL	BDL	0.18	15.84	4.99	4.77	9.59	BDL	1.63	BDL	0.69	BDL	BDL
BoC2d	60-80	16.32	BDL	BDL	0.18	16.63	6.93	4.26	6.84	BDL	BDL	BDL	0.86	BDL	BDL
BoC2e	80-100	22.69	BDL	BDL	0.22	19.58	4.64	6.22	5.53	BDL	BDL	BDL	0.82	BDL	BDL
BoC2f	100-120	19.51	BDL	BDL	0.19	20.46	5.00	8.47	5.14	BDL	BDL	BDL	0.95	BDL	BDL
BoC2g	120-140	22.83	BDL	0.06	0.25	14.64	4.51	15.99	2.54	BDL	1.68	BDL	0.96	BDL	BDL
BoC2h	140-160	24.66	BDL	0.08	0.33	18.29	5.89	18.04	1.59	BDL	2.02	BDL	0.85	BDL	BDL
BoC2i	160-180	37.45	BDL	0.12	0.37	16.78	5.91	22.73	3.03	BDL	1.92	BDL	0.56	BDL	BDL
BoC2j	180-200	170.51	BDL	0.11	0.46	17.05	11.39	75.12	6.60	BDL	4.56	BDL	0.44	BDL	BDL
Bod1k	0-2	12.40	BDL	BDL	BDL	117.71	14.76	4.44	1.14	BDL	2.81	BDL	2.31	0.51	1.13
Bod1L	9-11	5.78	BDL	0.07	BDL	92.22	10.61	2.38	0.58	BDL	2.07	BDL	1.87	1.01	1.77
Bod1a	0-20	11.67	BDL	0.07	BDL	90.65	12.38	3.70	1.45	BDL	2.71	0.04	1.88	0.69	0.30
Bod1b	20-40	10.93	BDL	0.16	BDL	120.28	13.83	3.98	1.52	BDL	2.89	0.07	2.79	0.64	0.42

Bod1c	40-60	8.47	BDL	0.17	BDL	78.09	21.71	3.15	2.50	BDL	3.27	0.09	3.06	0.51	0.37
Bod1d	60-80	4.30	BDL	0.11	BDL	34.30	4.11	1.51	1.99	BDL	2.13	BDL	2.52	0.16	BDL
Bod1e	80-100	4.66	BDL	0.06	BDL	21.50	7.10	1.36	1.27	BDL	2.26	BDL	2.80	BDL	BDL
Bod1f	100-120	6.49	BDL	0.12	BDL	37.57	6.95	2.11	3.12	BDL	3.81	BDL	4.71	0.21	BDL
Bod1g	120-140	4.81	BDL	0.12	BDL	37.73	5.24	2.22	2.90	BDL	2.62	0.04	4.00	BDL	BDL
Bod1h	140-160	5.09	BDL	0.11	BDL	46.29	5.32	2.40	3.01	BDL	2.45	0.05	4.26	BDL	BDL
Bod1i	160-180	10.74	BDL	0.14	BDL	45.24	7.72	3.45	3.67	BDL	3.47	0.15	4.85	BDL	0.25
Bod1j	180-200	7.60	BDL	0.12	BDL	28.52	3.62	1.64	1.53	BDL	2.72	0.08	2.37	0.10	0.23
Bod2k	0-2	8.77	BDL	BDL	BDL	73.37	7.19	2.30	1.07	BDL	2.69	BDL	1.62	0.90	2.93
Bod2L	9-11	6.56	BDL	0.08	BDL	76.98	6.31	2.34	5.63	BDL	2.87	BDL	2.13	1.41	2.31
Bod2a	0-20	10.41	BDL	0.15	BDL	78.39	9.96	2.48	8.93	BDL	3.28	0.06	3.88	0.66	0.66
Bod2b	20-40	7.05	BDL	0.08	BDL	40.72	5.69	1.53	4.59	BDL	2.99	0.09	3.17	0.08	0.23
Bod2c	40-60	3.90	BDL	BDL	BDL	26.60	3.05	0.96	1.71	BDL	2.05	BDL	2.83	BDL	BDL
Bod2d	60-80	4.72	BDL	0.10	BDL	71.78	2.79	1.90	2.10	BDL	2.42	BDL	6.56	0.05	BDL
Bod2e	80-100	6.67	BDL	0.17	0.37	111.95	4.09	2.95	4.50	BDL	6.50	0.34	11.08	0.05	0.48
Bod2f	100-120	12.65	BDL	0.11	0.20	76.26	7.52	3.04	5.42	BDL	9.25	0.09	16.05	0.05	0.32
Bod2g	120-140	7.86	BDL	0.05	BDL	44.83	4.73	1.79	2.83	BDL	4.47	0.16	12.22	BDL	0.25
Bod2h	140-160	2.83	BDL	BDL	BDL	18.11	2.32	0.90	1.10	BDL	BDL	BDL	5.39	BDL	BDL
Bod2i	160-180	4.18	BDL	BDL	BDL	20.10	2.81	1.18	1.13	BDL	BDL	BDL	7.22	BDL	BDL
Bod2j	180-200	5.88	BDL	BDL	BDL	20.48	4.49	1.50	1.82	BDL	4.42	BDL	7.63	BDL	BDL

Table S3.6: Soil nutrients by depth within the Hancock County site located in Newton, Georgia. (BDL= Below Detection Limit)

Jones Center (mg/kg)															
Sample Name	**Depth (cm)**	**Ca**	**Cd**	**Cr**	**Cu**	**Fe**	**K**	**Mg**	**Mn**	**Mo**	**Na**	**Ni**	**P**	**Pb**	**Zn**
TWC-1k	0-2	343.22	BDL	BDL	BDL	11.80	34.63	74.36	56.73	BDL	BDL	0.14	9.84	0.00	0.92
TWC-1L	9-11	39.48	BDL	BDL	BDL	14.47	15.48	13.68	10.95	BDL	2.32	0.16	1.72	0.04	0.30
TWC-1a	0-20	89.65	BDL	BDL	1.13	21.94	21.99	23.61	28.82	BDL	3.85	0.08	2.85	0.09	0.25
TWC-1c	40-60	59.52	BDL	BDL	BDL	20.97	9.69	28.86	18.97	BDL	2.65	0.08	0.92	0.06	BDL
TWC-1e	80-100	82.25	BDL	BDL	BDL	5.12	6.06	75.54	0.32	BDL	BDL	0.06	0.63	0.03	BDL
TWC-1g	120-140	9.55	BDL	BDL	BDL	4.29	5.15	29.77	BDL	BDL	2.24	0.10	0.47	0.13	BDL
TWC-1i	160-180	4.78	BDL	BDL	BDL	5.75	3.71	16.90	BDL	BDL	BDL	0.08	0.60	0.16	BDL
TWC-2k	0-2	420.31	BDL	BDL	BDL	11.81	30.63	82.42	40.53	BDL	2.67	0.17	10.67	0.00	0.66
TWC-2L	9-11	295.26	BDL	BDL	BDL	9.48	12.01	47.09	19.91	BDL	3.04	0.18	1.98	0.00	BDL
TWC-2a	0-20	199.36	BDL	BDL	0.22	11.83	12.52	37.35	22.18	BDL	3.70	0.09	2.98	0.05	0.26
TWC-2c	40-60	67.16	BDL	BDL	BDL	10.86	4.87	12.28	9.49	BDL	BDL	0.06	2.15	0.00	BDL
TWC-2e	80-100	46.47	BDL	BDL	BDL	6.74	5.37	10.04	2.75	BDL	BDL	0.06	2.90	0.00	BDL
TWC-2g	120-140	81.44	BDL	BDL	BDL	9.36	5.82	29.62	1.58	BDL	BDL	0.06	4.15	0.00	BDL
TWC-2i	160-180	144.74	BDL	BDL	BDL	8.38	6.98	68.49	BDL	BDL	2.44	0.07	1.99	0.00	BDL
TWC-3k	0-2	499.94	BDL	BDL	BDL	23.12	98.45	81.51	93.70	BDL	3.90	0.22	4.42	0.06	0.41
TWC-3L	9-11	28.80	BDL	BDL	BDL	20.35	9.16	15.02	22.16	BDL	2.14	0.15	1.30	0.00	BDL
TWC-3a	0-20	121.03	BDL	BDL	BDL	33.96	17.79	25.68	52.78	BDL	3.77	0.12	2.47	0.00	0.20
TWC-3c	40-60	22.60	BDL	BDL	BDL	12.36	4.90	16.42	14.19	BDL	2.10	0.08	1.34	0.00	BDL
TWC-3e	80-100	47.48	BDL	BDL	BDL	7.82	7.02	14.69	4.00	BDL	BDL	0.07	2.22	0.02	BDL
TWC-3g	120-140	50.51	BDL	BDL	BDL	6.20	21.10	21.23	1.25	BDL	BDL	0.05	3.53	0.07	BDL
TWC-3i	160-180	57.09	BDL	BDL	BDL	4.83	7.81	27.95	0.91	BDL	BDL	0.08	4.61	0.00	BDL
TWB-1k	0-2	748.36	BDL	BDL	BDL	12.33	40.48	150.51	55.65	BDL	2.59	0.25	10.15	0.05	0.69
TWB-1L	9-11	147.73	BDL	BDL	0.26	24.27	10.82	42.48	32.74	BDL	2.46	0.14	1.79	0.00	BDL
TWB-1a	0-20	362.48	BDL	BDL	BDL	15.04	13.99	74.46	34.81	BDL	2.67	0.10	2.98	0.00	0.37
TWB-1c	40-60	41.20	BDL	BDL	BDL	10.35	4.76	21.30	11.80	BDL	2.21	0.08	2.01	0.00	BDL

TWB-1e	80-100	44.31	BDL	BDL	BDL	7.77	5.56	16.80	4.76	BDL	BDL	0.07	2.53	0.02	BDL
TWB-1g	120-140	63.25	BDL	BDL	BDL	11.36	6.32	34.52	1.75	BDL	3.25	0.05	2.74	0.07	BDL
TWB-1i	160-180	84.44	BDL	BDL	BDL	6.69	7.72	59.32	0.21	BDL	BDL	0.05	2.11	0.02	BDL
TWB-2k	0-2	526.50	BDL	BDL	BDL	20.81	48.28	105.90	80.35	BDL	3.89	0.23	28.74	0.00	1.73
TWB-2L	9-11	114.79	BDL	BDL	0.20	52.04	12.06	27.16	59.59	BDL	BDL	0.22	6.63	0.01	BDL
TWB-2a	0-20	329.62	BDL	BDL	BDL	25.35	24.23	55.20	46.29	BDL	3.92	0.12	7.23	0.00	0.40
TWB-2c	40-60	29.63	BDL	BDL	BDL	12.90	4.68	13.54	9.45	BDL	BDL	0.06	2.06	0.00	BDL
TWB-2e	80-100	14.51	BDL	BDL	BDL	8.65	5.61	4.98	2.32	BDL	4.25	0.08	2.53	0.00	BDL
TWB-2g	120-140	15.42	BDL	BDL	BDL	9.43	4.64	7.03	1.71	BDL	BDL	0.05	4.02	0.00	BDL
TWB-2i	160-180	16.03	BDL	BDL	BDL	10.20	6.50	10.78	1.57	BDL	BDL	0.06	5.66	0.00	BDL
TWB-3k	0-2	266.56	BDL	BDL	BDL	14.60	36.50	45.49	26.72	BDL	2.52	0.20	4.73	0.02	0.49
TWB-3L	9-11	36.97	BDL	BDL	BDL	35.98	10.64	10.77	17.28	BDL	BDL	0.14	1.64	0.00	BDL
TWB-3a	0-20	137.02	BDL	BDL	BDL	20.27	13.60	21.32	15.98	BDL	2.58	0.08	2.08	0.00	0.30
TWB-3c	40-60	9.71	BDL	BDL	BDL	13.74	7.57	4.84	3.21	BDL	BDL	0.10	0.91	0.07	BDL
TWB-3e	80-100	14.19	BDL	BDL	BDL	12.64	8.00	32.57	0.28	BDL	2.98	0.08	0.87	0.07	BDL
TWB-3g	120-140	3.42	BDL	BDL	BDL	10.03	9.11	12.56	0.22	BDL	4.75	0.06	0.68	0.10	BDL
TWB-3i	160-180	3.21	BDL	BDL	BDL	8.67	9.28	5.18	0.27	BDL	3.93	0.08	0.72	0.09	BDL

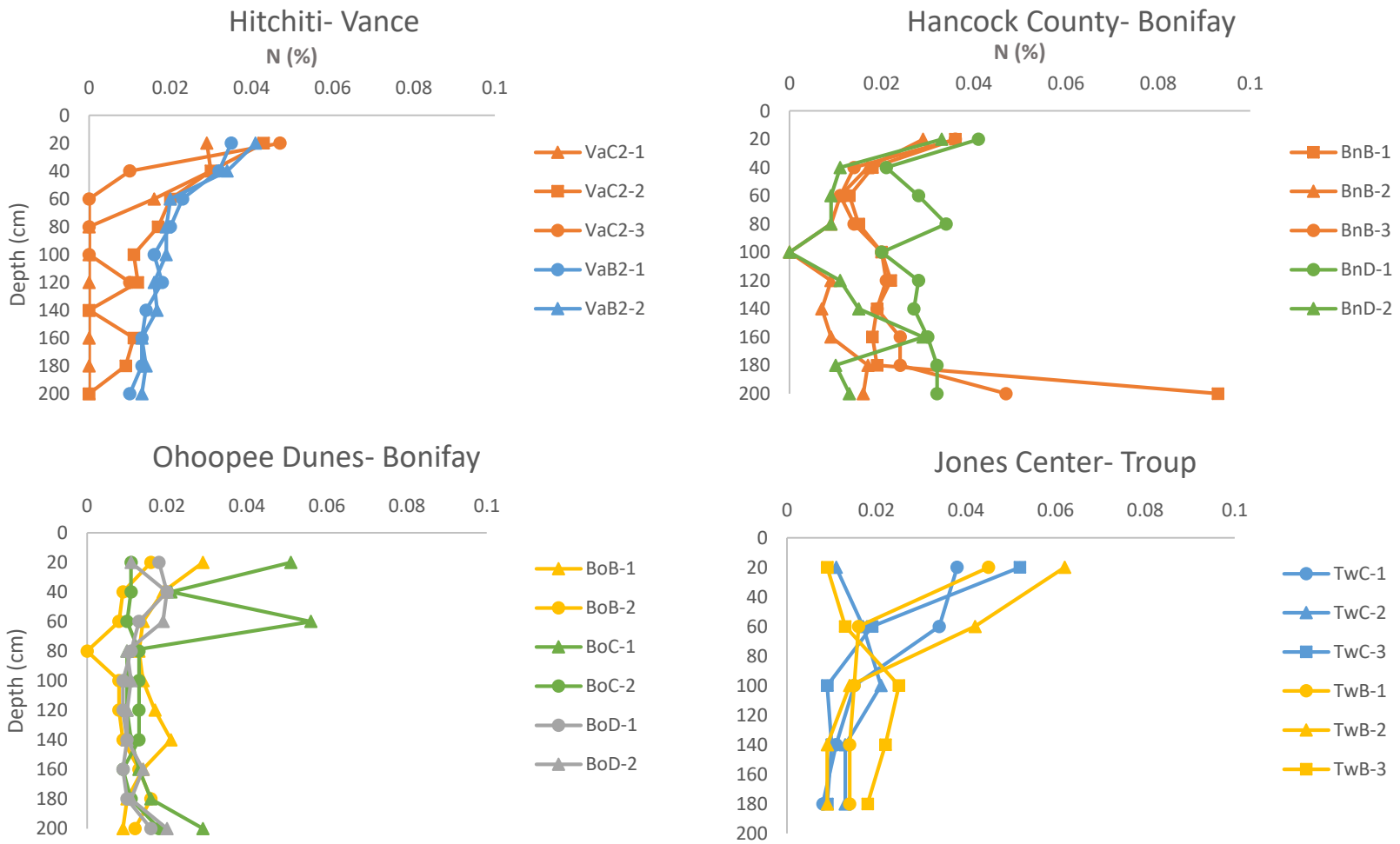

Figure S3.1. Indicates percent N for each site by depth and map unit. Within each graph, same color indicates same map unit and different shape indicates different soil profile within that map unit category. Collected 2015/2016.

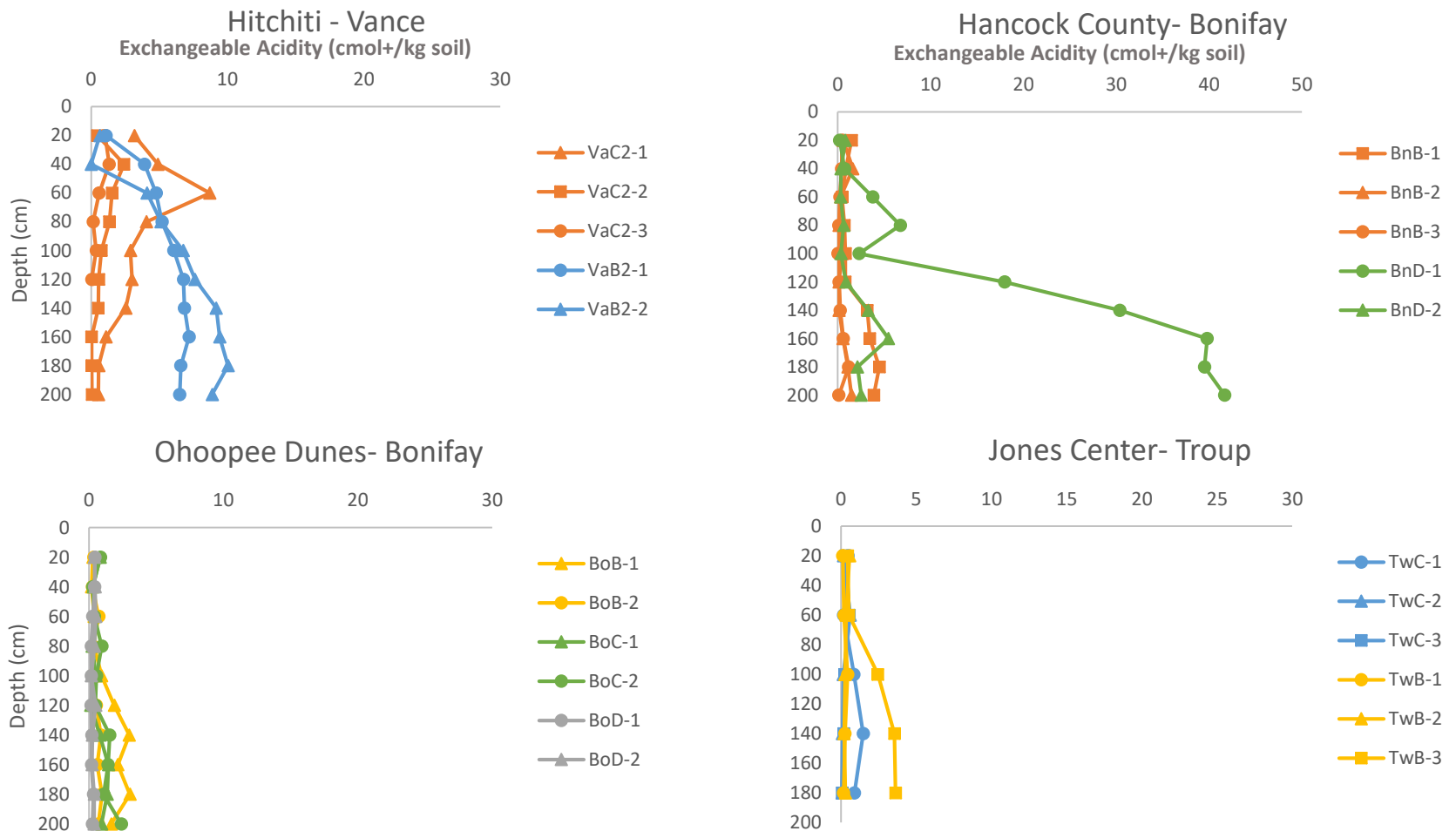

Figure S3.2. Indicates Exchangeable Acidity for each site by depth and map unit. Within each graph, same color indicates same map unit and different shape indicates different soil profile within that map unit category. Collected 2015/2016.